Quaternary International xxx (2009) 1–16

Contents lists available at ScienceDirect

Quaternary International

journal homepage: www.elsevier.com/locate/quaint

Paleoenvironmental and archaeological investigations at Qinghai Lake, western China: Geomorphic and chronometric evidence of lake level history

David Rhode [a,*], Ma Haizhou [b], David B. Madsen [c], P. Jeffrey Brantingham [d], Steven L. Forman [e], John W. Olsen [f]

[a] Earth and Ecosystem Sciences, Desert Research Institute, Reno, NV 89512, USA
[b] Qinghai Institute of Salt Lakes, Chinese Academy of Sciences, Xining, Qinghai 810008, PR China
[c] Texas Archeological Research Laboratory, University of Texas, Austin, TX 78712, USA
[d] Department of Anthropology, University of California Los Angeles, Los Angeles, CA 90095, USA
[e] Department of Earth and Environmental Sciences, University of Illinois at Chicago, Chicago, IL 60607, USA
[f] Department of Anthropology, University of Arizona, Tucson, AZ 85721, USA

A B S T R A C T

Qinghai Lake, located on the northeastern Qinghai–Tibet Plateau (Qing-Zang Gaoyuan), is China's largest extant closed-basin lake. Its position relative to major Asian climate systems makes it sensitive to global climate change. The lake has been the subject of numerous paleoenvironmental investigations including dating of shoreline features around the lake basin. Here we report new age estimates of shoreline features, geomorphic exposures and archaeological sites that contribute to the development of a lake-level history for Qinghai Lake and a landscape model of the Qinghai Lake Basin. Lake highstands above 3230 m (~36 m above the modern lake level) appear to date to late MIS 5, ~70–110 ka. The lake has had much more modest highstands since then: no evidence of MIS 3 lake stands higher than modern were found, and early Holocene highstands are no more than ~12 m above modern. If the age of highstands greater than 3230 m is confirmed through future work, then the Qinghai Lake Basin hydrologic balance prior to ~70 ka was dramatically different than after that time, including during the Holocene. A simple hydrologic balance model provides insights into the combination of precipitation, evaporation, and runoff generation needed to sustain the lake at 3260 m, the highest shoreline observed. A range of factors may explain the difference, primarily the relative strength of the East Asian monsoon. The basin was apparently subject to extensive alluviation during MIS 3, interrupted by widespread erosion and development of cryogenic features before and during the last glacial maximum (LGM). Loess that presently drapes much of the lower basin landscape began to be deposited after the LGM, ~16–18 ka. The landscape model outlined here has implications for archaeological visibility of early human occupation of the Qinghai–Tibet Plateau.

1. Introduction

The Qinghai–Tibet Plateau ranks among the most challenging terrestrial habitats on earth for human occupation. Extreme altitude, severe climate, and scant resources all served as effective constraints to early humans who tested the idea of living on the 'roof of the world.' By the early Holocene, though, people had found ways to make a living in the harsh Qinghai–Tibet Plateau environment above 4500 m (and other high-elevation plateaus in other parts of the world; Aldenderfer, 2003, 2006). An important step in this process of adjustment to life on the high Qinghai–Tibet Plateau was successful habitation of slightly lower altitudes on its margins, a step that people apparently took first during the late Pleistocene.

The place where this process is best documented archaeologically is the Qinghai Lake Basin, on the northeastern fringe of the Plateau (Fig. 1). Evidence of Upper Paleolithic human occupation is known from the Qinghai Lake Basin dating from the terminal Pleistocene, and putatively older materials have been reported in the neighboring Qaidam Basin to the west (Huang, 1994; Huang and Hou, 1998; but cf. Brantingham et al., 2007). To obtain evidence regarding when modern humans first entered the northeastern Qinghai–Tibet Plateau, the Qinghai Lake Basin seemed an excellent place to begin. We have recently investigated the archaeological

* Corresponding author. Tel.: +1 775 673 7310.
E-mail address: dave.rhode@dri.edu (D. Rhode).

1040-6182/$ – see front matter © 2009 Elsevier Ltd and INQUA. All rights reserved.
doi:10.1016/j.quaint.2009.03.004

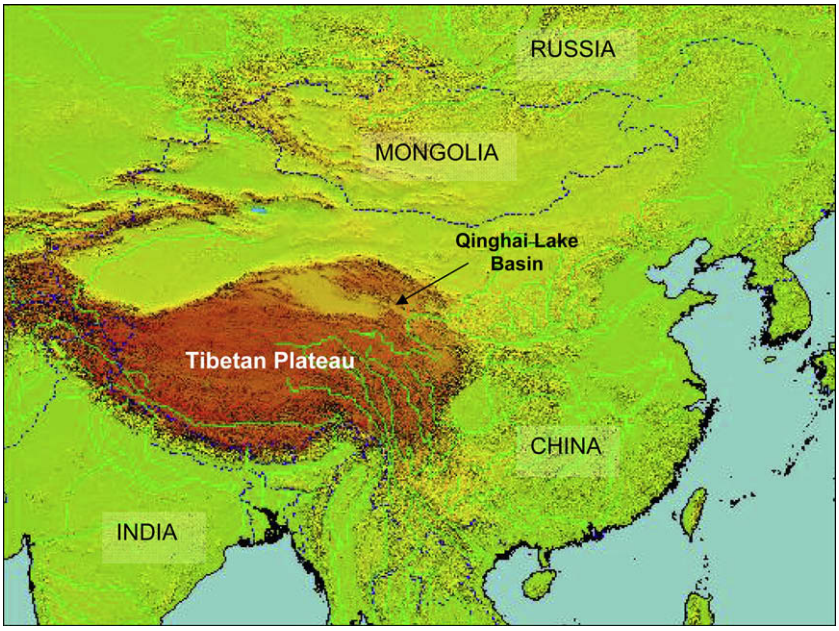

Fig. 1. Location of Qinghai Lake Basin on the northeast Qinghai–Tibet Plateau.

evidence for this early human occupation (Brantingham et al., 2003, 2007; Brantingham and Gao, 2006; Madsen et al., 2006; Rhode et al., 2007). In so doing we are also concerned with the environmental history of Qinghai Lake itself, to establish the environmental context of early human colonization and to guide our decisions about which localities and exposed sediments are most likely to contain archaeological evidence of the right time period (Brantingham et al., 2003, 2007; Madsen et al., 2007).

To those ends, we recently investigated the environmental history of the Qinghai Lake Basin directed particularly toward the exposed shoreline history of the lake and the timing of deposition of loess and other deposits (Madsen et al., 2008). This paper summarizes our findings to date.

2. Setting

Qinghai Lake (also known as Koko Nor in Mongolian, and mTsho sngon po in Tibetan) is presently the largest extant closed-basin lake in China, one of the largest in Central Asia. It lies on the northeastern Qinghai–Tibet Plateau between 36.3°–38.3° N and 97.9°–101.3° E (Fig. 2), the terminus of a ~29,660 km^2 catchment (LZBCAS, 1994). The lake basin was formed during the late Miocene

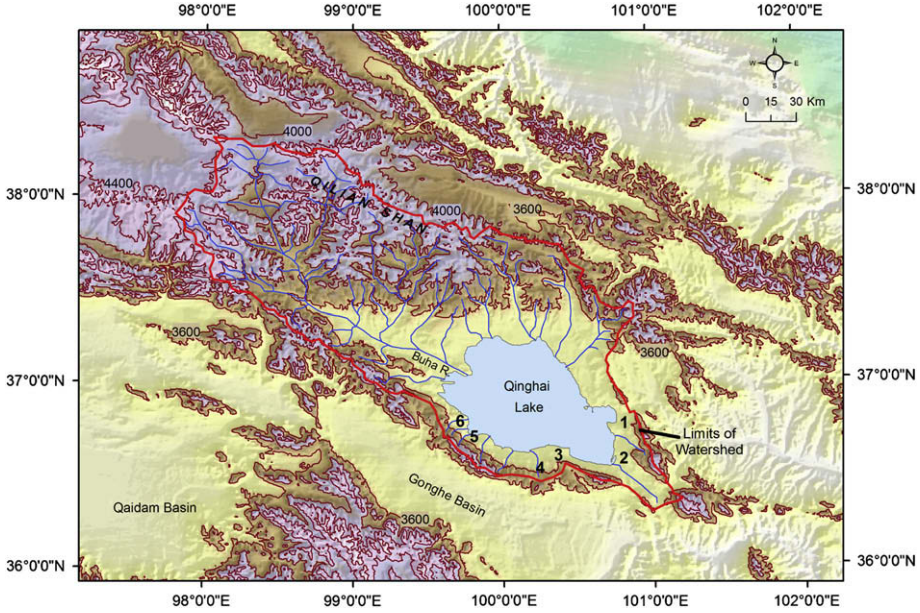

Fig. 2. Qinghai Lake and its watershed. Paleolake localities are numbered. 1: Paleoshoreline deposits and barrier bar/lagoon deposits at 3240–3245 m elevation east of Haiyin Bay, west side of Ketu Pass. 2: Spit and paleoshoreline complex at 3245–3260 m elevation north of Daotang River, south of Riyue Mountains. 3: Alluvial gravels, periglacial wedges, and lacustrine sand deposits exposed in gravel pits on south side of lake. 4: Periglacial wedges in fan deposits, upper Jiangxigou Creek. 5: Archaeological sites at Heimahe. 6: Road cuts northwest of Heimahe.

Please cite this article in press as: Rhode, D., et al., Paleoenvironmental and archaeological investigations at Qinghai Lake, western China:..., Quaternary International (2009), doi:10.1016/j.quaint.2009.03.004

and Pliocene as part of the uplift of the northeastern Qinghai–Tibet Plateau (Métivier et al., 1998; An et al., 2001; Fang et al., 2005; Harris, 2006; Wang et al., 2008), originally forming a headwater basin feeding the proto-Yellow River. Tectonic uplift of the Riyue Mountains closed the basin at the southeastern and eastern ends during the Middle to Late Pleistocene (Yuan et al., 1990; Pan, 1994; Li and Fang, 1999).

The lake has a surface altitude of ~3194 m (measured in 1986) and a surface area of ~4300 km^2, about one-seventh of its basin size. Surrounding mountains typically exceed 4000 m, reaching above 5000 m in the northwest basin; the highlands make up ~70% of the drainage area. The region's climate is cold and semi-arid, with a mean annual temperature of −0.7 °C subject to high seasonal differences (~12 °C in summer, −11 °C in winter). Mean annual evaporation is approximately ~925 mm (1959–2000), with a gradient of ~1000 mm at the lake surface to ~300 mm in the surrounding mountains (Colman et al., 2007). Estimates of mean annual precipitation range from ~250–400 mm, with an average value of ~360 mm and significant variability over the watershed (Walker, 1993; Qin, 1997; Qin and Huang, 1998; Yan et al., 2002; Shen et al., 2005; Yu, 2005; Colman et al., 2007; Li et al., 2007). Mean annual precipitation results in ~1.57×10^9 m^3 of direct input to Qinghai Lake's water balance (LZBCAS, 1994; Li et al., 2007). Approximately 60% of annual precipitation falls during June–August, derived from storms generated by the East Asian Monsoon.

Dozens of drainages debouch into Qinghai Lake, but most are intermittent and typically dry. Five main permanent streams provide over 80% of total surface inflow, the Buha River being the largest contributor with ~49% of the total (Fig. 2). Average annual surface inflow into Qinghai Lake is estimated at ~1.5×10^9 m^3, resulting in ~320–350 mm input to the current lake area (Walker, 1993; LZBCAS, 1994; Xu et al., 2006; Li et al., 2007). Average annual groundwater inflow contributes an additional 0.6×10^9 m^3, ~140 mm input to current lake area (Lanzhou Institute of Geology, 1979; Yu and Kelts, 2002; Li et al., 2007).

A combination of high evaporation and reduced precipitation and surface inflow has resulted in a recent net loss of lake level of ~80 mm/yr (Qin and Huang, 1998; Yan et al., 2002; Li et al., 2007), causing concern about the viability of the lake and its wildlife, including the endangered endemic naked carp *Gymnocypris przewalskii* (Walker, 1993; Qu, 1994). The decline of lake level appears to be primarily the result of increasing temperature in the late twentieth century, though recent human use has contributed a small but significant depletion (Li et al., 2007).

The Qinghai Lake watershed is positioned near the edge of influence of the East Asian and Southwest Asian summer monsoons, and also lies within the path of prevailing continental dry westerlies from northern Eurasia, as modulated and amplified by the influence of the Qinghai–Tibet Plateau itself (Lister et al., 1991; Benn and Owen, 1998; Lu et al., 2004; Herzschuh, 2006; Vandenberghe et al., 2006). Fluctuations in the strength and position of these climatic regimes alters the amount of precipitation, and hence runoff, in the watershed (Ji et al., 2005; Herzschuh, 2006; Herzschuh et al., 2006). The high sensitivity of lake levels to changes in temperature and precipitation (Qin and Huang, 1998), and its position with respect to these global-scale atmospheric systems, has made it attractive for studies of paleoclimatic change on the Qinghai–Tibet Plateau, most involving climatic proxies derived from sediment cores from the lake itself (Kelts et al., 1989; Chen et al., 1990; Yuan et al., 1990; Lister et al., 1991; Wang and Li, 1991; Wang et al., 1991; Wang and Shi, 1992; Liu et al., 2002; Yu and Kelts, 2002; Ji et al., 2005; Shen et al., 2005; Yu, 2005; Colman et al., 2007). Other studies have focused on the history of fluctuating lake levels from exposed shorelines and other features (Chen et al., 1990; Yuan et al., 1990; Wang et al., 1991; Wang and Shi, 1992; Porter et al., 2001; Zhang et al., 2004a). These studies have reported past shoreline features from 10 to as much as 140 m above modern lake levels, indicating dramatic shifts in lake level resulting from Quaternary climate change (Fig. 3).

3. Methods

3.1. Field reconnaissance

Localities investigated in the Qinghai Lake Basin were mapped using a combination of satellite-based geographic positioning systems, accurate to within a few meters, 1:50,000 scale topographic maps, and Google Earth satellite imagery. Altitudes were obtained using the same topographic maps with contour intervals

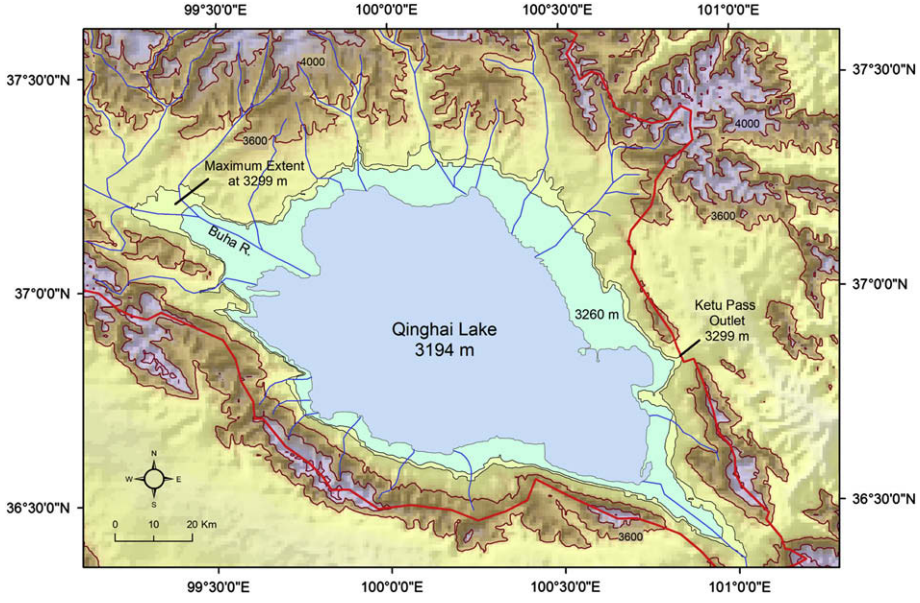

Fig. 3. Surface areas for Qinghai Lake at the modern 3194 m altitude (blue), 3260 m (blue-green), and 3299 m, when it overflows through Ketu Pass (olive).

Please cite this article in press as: Rhode, D., et al., Paleoenvironmental and archaeological investigations at Qinghai Lake, western China:..., Quaternary International (2009), doi:10.1016/j.quaint.2009.03.004

spaced 10 m apart, Google Earth imagery, and with barometric altimeters set to known altitudes.

3.2. Dating

We used radiocarbon age estimates where organic materials in reliable context were available, predominantly in archaeological sites. We used optically-stimulated luminescence (OSL) to date shoreline sediments beyond the range of radiocarbon dating and where organic remains were not present. Age estimates newly derived for this paper are given in Table 1. Age estimates we have previously reported (Madsen et al., 2008) are provided in Table 2.

Luminescence dating of sediments was completed on the fine-grained (4–11 m) polymineral and coarse-grained (100–250 m) quartz fractions. All samples were dated by the multiple aliquot regeneration (MAR) dose procedures, using component-specific dose normalization (CSDN) method (Forman and Pierson, 2002; Jain et al., 2003). Initially, the CSDN procedure determined equivalent dose with infrared (IR) stimulation and subsequently with green or blue light excitation. The sequence of OSL analysis (IR followed by green or blue light excitation) preferentially measures feldspar-sourced and then quartz emissions. The fine-grained polymineral extract was also analyzed by the multiple aliquot additive dose (MADD) methods, under infrared stimulation (880 ± 80 nm), by an automated Daybreak 1100 reader (Forman and Pierson, 2002; Jain et al., 2003). MAR analyses were completed under green (514 ± 20 nm) or blue (470 ± 20 nm) light excitation by a Daybreak reader. The resultant blue emissions were measured at ~25 °C by a photomultiplier tube coupled with one 3-mm-thick Schott BG-39 and one 3-mm-thick Corning 7-59 glass filters; these emissions are the most suitable as a chronometer (Balescu and Lamothe, 1992; Lang et al., 2003). The background count rate for measuring emissions was <100 counts/s, with a signal-to-noise ratio of >20. A sample was excited for 90 s, and the resulting emissions was recorded in 1 s increments.

With two exceptions (UIC1658 and UIC1868), ages determined by IR and green- or blue-light excitation overlap at 2-sigma and thus are statistically similar. We favor the ages determined by green or blue light because quartz is a well-known and robust geochronometer, though of less temporal utility than feldspar (Prescott and Hutton, 1994). As a result, we use the green or blue ages for interpretive purposes. However, because of the general concordance of IR and green and blue ages, when green-excitation yields infinite ages the finite IR age is considered an appropriate age

Table 1
Optically stimulated luminescence (OSL) ages and associated chronologic data for sediments from Qinghai Lake area, reported in this paper.

Locality	Field number	Laboratory number	Equivalent dose	*A* value[d]	Uranium	Thorium	K_2O	Cosmic dose	Total dose rate	OSL age
			(Grays)		(ppm)[e]	(ppm)[e]	(%)[e]	(mGrays/yr)	(mGrays/yr)[f]	(yr)[g]
North Shore Gravel Pit	FS06-05	UIC1829IR	>277.71 ± 27.0[c]	NA	1.2 ± 0.1	5.3 ± 0.1	2.42 ± 0.02	0.25 ± 0.02	2.73 ± 0.10	>101,865 ± 12,720
North Shore Gravel Pit	FS06-05	UIC1829Bl	>310.00 ± 30.0[c]	NA	1.2 ± 0.1	5.3 ± 0.1	2.42 ± 0.02	0.25 ± 0.02	2.73 ± 0.10	>113,700 ± 14,160
East Side Sand Spit Complex	FS07-51	UIC2175Bl	169.05 ± 9.39[c]	NA	1.2 ± 0.1	5.4 ± 0.1	1.93 ± 0.01	0.19 ± 0.02	2.29 ± 0.11	73,750 ± 6750
South Shore Km 2117 Pit	FS07-05	UIC2177Bl	383.63 ± 2.60	0.08 ± 0.01	2.7 ± 0.1	11.1 ± 0.1	2.14 ± 0.02	0.20 ± 0.00	4.26 ± 0.20	90,080 ± 6700
South Shore Km 2117 Pit	FS07-05	UIC2177IR	434.28 ± 3.45	0.06 ± 0.01	2.7 ± 0.1	11.1 ± 0.1	2.14 ± 0.02	0.20 ± 0.00	4.06 ± 0.19	106,980 ± 7840
South Shore Km 2117 Pit	FS07-04	UIC2176Bl[a]	383.74 ± 2.99	0.08 ± 0.01	2.1 ± 0.1	9.4 ± 0.1	2.15 ± 0.01	0.20 ± 0.02	3.88 ± 0.16	98,950 ± 7400
South Shore Km 2117 Pit	FS07-04	UIC2176IR[b]	424.56 ± 3.61	0.07 ± 0.01	2.1 ± 0.1	9.4 ± 0.1	2.15 ± 0.01	0.20 ± 0.02	3.79 ± 0.16	111,950 ± 8330
Heimahe #1, 49 cmbs	FS04-93	UIC1568IrA[c]	27.35 ± 0.11	0.07 ± 0.01	2.4 ± 01	10.1 ± 0.1	1.97 ± 0.02	0.36 ± 0.04	3.91 ± 0.16	6995 ± 520
Heimahe #1, 92 cmbs	FS04-92	UIC1570IrA[c]	45.66 ± 0.10	0.07 ± 0.01	2.4 ± 0.1	9.1 ± 0.1	1.76 ± 0.02	0.34 ± 0.03	2.98 ± 0.11	15,310 ± 1080
Heimahe #1, 134 cmbs	FS04-91	UIC1566IrA[c]	56.95 ± 0.12	0.07 ± 0.01	2.3 ± 0.1	9.1 ± 0.1	2.04 ± 0.02	0.30 ± 0.03	3.81 ± 0.16	14,940 ± 1115
Heimahe #1, 159 cmbs	FS04-27	UIC1567IrA[c]	51.26 ± 0.10	0.10 ± 0.01	2.6 ± 0.1	10.4 ± 0.1	2.05 ± 0.02	0.32 ± 0.03	4.35 ± 0.18	11,785 ± 880
Heimahe #1, 234 cmbs	FS04-26	UIC1569Gr	110.50 ± 0.93	0.10 ± 0.01	2.4 ± 0.1	9.4 ± 0.1	2.10 ± 0.02	0.28 ± 0.03	4.16 ± 0.17	26,550 ± 1770
Heimahe #1, 234 cmbs	FS04-26	UIC1569Ir	75.40 ± 0.16	0.05 ± 0.01	2.4 ± 0.1	9.4 ± 0.1	2.10 ± 0.02	0.28 ± 0.03	3.70 ± 0.16	20,350 ± 1540
Heimahe #1, 234 cmbs	FS04-26	UIC1569IrA[c]	84.01 ± 0.21	0.06 ± 0.01	2.4 ± 0.1	9.4 ± 0.1	2.10 ± 0.02	0.28 ± 0.03	3.80 ± 0.16	22,130 ± 1670
Heimahe Road cut 1, 127 cmbs	FS05-38	UIC1657IrA[c]	6.27 ± 0.02	0.07 ± 0.01	2.4 ± 0.1	10.7 ± 0.1	2.31 ± 0.02	0.32 ± 0.03	4.23 ± 0.20	1555 ± 110
Heimahe Road cut 1, 173 cmbs	FS05-37	UIC1656IrA[c]	45.28 ± 0.11	0.07 ± 0.01	2.3 ± 0.1	9.1 ± 0.1	1.91 ± 0.02	0.30 ± 0.03	3.68 ± 0.13	12,300 ± 870
Heimahe Road cut 1, 290 cmbs	FS05-35	UIC1658Bl	515.63 ± 3.39	0.09 ± 0.01	2.3 ± 0.1	7.3 ± 0.1	2.25 ± 0.02	0.25 ± 0.02	3.88 ± 0.15	133,060 ± 10,000

[a] Equivalent dose determined by the multiple aliquot regenerative dose method under green excitation (514 nm) (Jain et al., 2003).
[b] Equivalent dose determined by the multiple aliquot regenerative dose method under infrared excitation (880 nm) (Jain et al., 2003).
[c] Equivalent dose determined by the multiple aliquot additive dose method under infrared excitation (880 nm) (e.g. Forman and Pierson, 2002). Blue emissions are measured with 3-mm-thick Schott BG-39 and one, 3-mm-thick Corning 7-59 glass filters that blocks >90% luminescence emitted below 390 nm and above 490 nm in front of the photomultiplier tube. Fine-grained (4–11 μm) polymineral fraction analyzed.
[d] Measured alpha efficiency factor as defined by Aitken and Bowman (1975).
[e] U and Th values calculated from alpha count rate, assuming secular equilibrium. K_2O% determined by ICP-MS, Activation Laboratory Ltd., Ontario.
[f] Contains a cosmic rate dose rate component from Prescott and Hutton (1994). A moisture content of 15 ± 5% was assumed.
[g] All errors are at one sigma. Analyses performed by Luminescence Dating Research Laboratory, Dept. of Earth & Environmental Sciences, Univerity of Illinois–Chicago.

Please cite this article in press as: Rhode, D., et al., Paleoenvironmental and archaeological investigations at Qinghai Lake, western China:..., Quaternary International (2009), doi:10.1016/j.quaint.2009.03.004

Table 2
Optically stimulated luminescence (OSL) ages from Qinghai Lake area reported in Madsen et al. (2008).

Locality	Field number	Laboratory number	OSL age (yr)[e]
North Shore Gravel Pit	FS06-05	UIC1829IR[b,d]	102540 ± 7835
South Shore Km 2117 Pit	FS06-46	UIC1827IR[d]	18640 ± 1500
South Shore Km 2117 Pit Ground Wedge	FS05-166	UIC1652Gr[d]	22640 ± 1790
South Shore Km 2114.5 Pit	FS06-47	UIC1868GR[d]	38840 ± 2955
South Shore Km 2114.5 Pit	FS06-47	UIC1868IR[d]	53700 ± 4040
South Shore Km 2114.5 Pit	FS06-48	UIC1828GR	93270 ± 7080
South Shore Km 2114.5 Pit	FS06-48	UIC1828IR	96900 ± 7355
Jiangxigou Ground Wedge	FS05-127	UIC1651Gr	98370 ± 7390
Jiangxigou Ground Wedge	FS05-127	UIC1651Ir	102910 ± 7755
Jiangxigou Ice Wedge Cast	JXG10E W	UIC1573IrA[c]	≥41000 ± 3060
Jiangxigou Ice Wedge Cast	JXG10E W	UIC1573Gr	45560 ± 3390
Heimahe Road cut 1, 248 cmbs	FS05-36	UIC1659IrA[c]	16080 ± 1215
Heimahe Road cut 1, 248 cmbs	FS05-36	UIC1659Ir	17920 ± 1350
Heimahe Road cut 1, 248 cmbs	FS05-36	UIC1659Gr	17935 ± 1350
Heimahe Road cut 1, 290 cmbs	FS05-35	UIC1658Ir	94455 ± 7110
Heimahe Road cut 2	FS06-45	UIC1830GR[a]	24970 ± 1850
Heimahe Road cut 2	FS06-45	UIC1830IR[a]	25800 ± 1910

[a] Equivalent dose determined by the multiple aliquot regenerative dose method under green excitation (514 nm) (Jain et al., 2003).
[b] Equivalent dose determined by the multiple aliquot regenerative dose method under infrared excitation (880 nm) (Jain et al., 2003).
[c] Equivalent dose determined by the multiple aliquot additive dose method under infrared excitation (880 nm) (e.g. Forman and Pierson, 2002). Blue emissions are measured with 3-mm-thick Schott BG-39 and one, 3-mm-thick Corning 7-59 glass filters that blocks >90% luminescence emitted below 390 nm and above 490 nm in front of the photomultiplier tube. Fine-grained (4–11 μm) polymineral fraction analyzed.
[d] The coarse fraction 150–250 or 100–150 μm quartz fraction is analyzed.
[e] All errors are at one sigma. Analyses performed by Luminescence Dating Research Laboratory, Dept. of Earth & Environmental Sciences. University of Illinois–Chicago.

estimate, and for sample UIC1829 we use IR ages for interpretive purposes.

A critical analysis for luminescence dating is the dose rate, which is an estimate of the sediment exposure to ionizing radiation during the burial period (Aitken and Bowman, 1975). Most ionizing radiation in sediment is from the decay of isotopes in the U and Th decay chains and ^{40}K, which was determined by inductively coupled plasma-mass spectrometry. A small cosmic ray component is included in the estimated dose rate (Prescott and Hutton, 1994). The dose rate also compensated for moisture content estimates at each site.

3.3. Lake water balance modeling

We used Arcmap and a GTOPO90 digital elevation model with 1 km resolution to estimate surface areas of lakes that would fill the Qinghai Lake Basin to different depths above 3205 m. Present-day lake surface area was set at 4300 km^2, following the reported cluster of estimates around this value (Lister et al., 1991; Qin and Huang, 1998; Henderson et al., 2003; Yan and Jia, 2003; Li et al., 2007). Surface areas for different lake depths in the Qinghai Lake Basin are given in Table 3.

We used the following simple water balance model to derive estimates of evaporation and precipitation needed to reach equilibrium surface areas:

$$A_L = (Q + G + M)/(E_L - P_L)$$

where A_L is lake surface area (in m^2), Q is surface inflow (in m^3), G is groundwater flow (m^3), M is inflow from glacial melt, E_L is evaporation from the lake (m), and P_L is precipitation on the lake (m). We assume G is constant $= 6.0 \times 10^8$ m^3/yr (Li et al., 2007), regardless of lake depth. For this exercise we assume that M, glacial meltwater, is negligible; Yu and Kelts (2002) reported it to be ~1% of total surface inflow.

We want Q, surface inflow, to be a function of P_L, such that

$$Q = A_D{*}k{*}P_L$$

where A_D is the drainage area excluding the lake area (i.e., $A_D = 29{,}660 - A_L$), and k is a coefficient expressing the proportion of inflow per unit A_D, compared to P_L. To obtain an estimate for k, we calculated the relationship between total surface inflow to the lake and precipitation on the lake using data from 1970–1990 (Walker, 1993). The correlation between total surface inflow and lake precipitation shows considerable scatter (Fig. 4), but the relationship appears linear and reasonably strong ($r^2 = 0.55$). Comparing the amount of precipitation falling on the lake to the amount of surface inflow generated per unit area of the drainage basin gives a current value of $k = \sim 0.141$, with a standard deviation of 0.048 and a range of 0.063–0.230.

We approach modeling in two ways. For a known elevation we define A_L and find combinations of values for E_L, P_L, and k that satisfy A_L. This approach shows the sensitivity of evaporation, precipitation, and runoff generation on lake water balance (Fig. 5). We also examine how lake surface area changes by holding k constant (at 0.141) and varying evaporation and precipitation (Fig. 6). This approach provides a useful comparison of the water balance needed to support higher lakes compared to modern conditions. Using both approaches we can delimit a likely range of hydrologic conditions for paleolake levels.

Table 3
Estimated surface area and inflowing drainage basin area for different lake levels in the Qinghai Lake Basin.

Lake level	Estimated surface area (km^2)	Inflowing drainage basin (km^2)	% of Total watershed	% of modern lake area
3194	4300	25360	14.5	–
3206	5466	24194	18.4	127
3245	6621	23039	22.3	154
3260	6952	22708	23.4	162
3299 (overflow)	7655	22005	25.8	178

Please cite this article in press as: Rhode, D., et al., Paleoenvironmental and archaeological investigations at Qinghai Lake, western China:..., Quaternary International (2009), doi:10.1016/j.quaint.2009.03.004

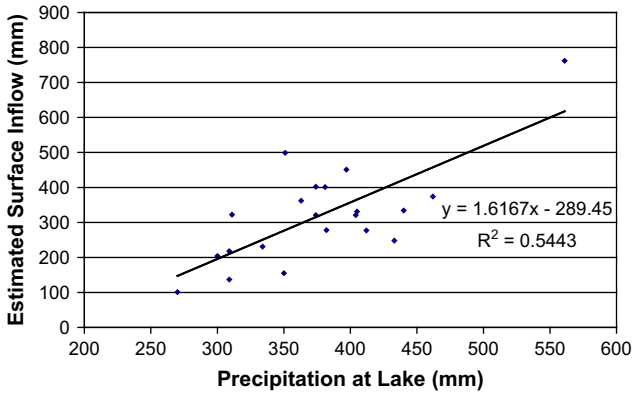

Fig. 4. Correlation of precipitation measured at lakeshore stations near Qinghai Lake (Heimahe, Yao Wuyao, and Sha Tueshi) and estimated total surface runoff into the lake. Data from Walker, 1993 (table 3.2) for the years 1970–1990.

4. Localities

4.1. Northeast shore gravel pit and shoreline complex

A series of well developed paleoshorelines and a barrier bar feature are located on Qinghai Lake's northeast shore (36.821° N, 100.794° E; Fig. 2), previously described by Madsen et al. (2008). The highest of these paleoshoreline features, readily visible on satellite imagery and in the field, are exposed in a road cut at 3245–3250 m (Fig. 7). Heavily pedogenically carbonate-coated shoreline gravels are capped by overlying surface loess of Holocene age. The shoreline gravels are truncated by an erosional unconformity that has removed all but the base of a well-developed soil weathered into the gravels. These shorelines are presently undated.

At a slightly lower elevation of ~3240 m, a barrier bar complex is exposed in a gravel pit (Fig. 8). The uppermost stratum at this locality is blocky post-LGM/Holocene silt loess up to 1.5 m thick, with incipient soil development on the surface and possible paleosols at the base and middle of the unit. Beneath this surface loess are gravel and sand deposits, in places modified by periglacial activity to form involutions and ground wedges that are filled with the later Holocene loess. In one well-exposed section, coarse to medium gravels with finer sand and gravel lenses and stringers dip northeastward (away from the lake) as a series of foreset beds at a fairly steep angle. Erosion of the surface of these foreset beds has produced an unconformity truncating the bedding and removing all but the base of a well-developed soil. These foreset beds, approximately 1.5 m thick, extend over underlying fine-grained flat-bedded lagoon deposits. These deposits consist of laminated fine to medium sands between units of clayey sand containing unbroken ostracodes. In places these lagoon deposits are locally deformed. A fine sandy gravel layer <10 cm thick, beneath the clayey sand lagoon deposits, grades to a deposit of horizontally bedded fine- to medium-sized waterlain gravels reaching a maximum of 1.3 m thick approximately 50 m southeast of the lagoon deposits. Beneath this horizontally-bedded gravel layer is coarse angular alluvium with a well-developed paleosol on its surface.

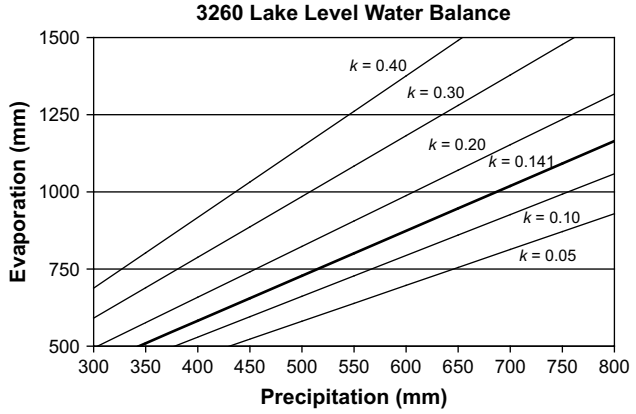

Fig. 5. Relation of variation in evaporation, precipitation, and surface inflow coefficient on water balance for Qinghai Lake at the 3260 m level. Note that for a given evaporation rate, a change in the runoff coefficient has a dramatic effect on the precipitation required to maintain the lake's level at 3260 m.

This sequence indicates a beach sequence with a back-barrier lagoon overtopped by transgressing beach gravels. From the lagoonal sands below the foreset gravels, we obtained a finite OSL age estimate of ~102.5 ± 7.8 ka (Madsen et al., 2008). Two new age estimates, from the same sample (UIC1829) but using different measurement protocols, yielded limiting ages of ~>101 and >113 ka (Table 1). A radiocarbon date of ~41 ^{14}C ka on clean whole ostracode shells from the underlying clayey sands is considered to be a limiting age of a deposit that is likely much older. These dates suggest that the 3240–3250 beach and shoreline complex is older than ~100 ka.

4.2. East shore beach and spit features

An extensive paleoshoreline and spit complex is located on the extreme eastern margin of the lake, on a bluff south of the Riyue Mountains and north of the Daotang River (36.495° N, 100.847° E; Fig. 2; cf. Madsen et al., 2008). This complex provided the highest Pleistocene shorelines we could securely identify in satellite imagery and in field examinations conducted over four seasons of fieldwork (Fig. 9). Two distinct wave-cut benches are located on a broad constructional terrace at altitudes of ~3250 and ~3260 m. No higher shorelines or wave-cut benches were observed on the well-exposed slopes to the immediate north, suggesting that higher lake levels may not have been attained. A prominent sand spit complex, presently used as a construction borrow pit, was formed at a maximum elevation of 3248 m. We obtained an OSL age of 73.7 ± 6.7 ka (UIC2175, Table 1) for this spit feature, approximately the end of MIS Stage 5a.

4.3. South shore gravel pits

A series of exposures in gravel pits along the highway on the southern margin of Qinghai Lake provide evidence of former higher lake levels, subsequent alluviation, and development of periglacial features on the Erlangjiang Terrace, the bajada fronting the Qinghai Nan Mountains (Fig. 2). This area was previously investigated by Wang and Shi (1992) and Porter et al. (2001). We have previously described some of these sections elsewhere (Madsen et al., 2008), but new dates and exposures are presented here.

One gravel pit at 3246 m altitude (36.601° N, 100.400° E, Km 2117 on the highway) contained several periglacial features exposed within coarse gravel alluvial fan deposits, below which lay a thick bed of lacustrine nearshore sand deposits (Fig. 10). The upper ~1–2 m of this section is blocky Holocene loess, deposited on top of ~1.7 m of poorly sorted cobbly alluvium with angular clasts up to 25 cm in diameter. This upper alluvium rests on the weathered, undulating and slightly westward-dipping surface of another lower alluvial deposit. This lower alluvial gravel unit, also ~1.7 m thick, consisting of poorly to moderately sorted angular cobbles to ~10 cm maximum dimension. Ice/sand wedges extend down into it from the undulating surface between the upper and

Please cite this article in press as: Rhode, D., et al., Paleoenvironmental and archaeological investigations at Qinghai Lake, western China:..., Quaternary International (2009), doi:10.1016/j.quaint.2009.03.004

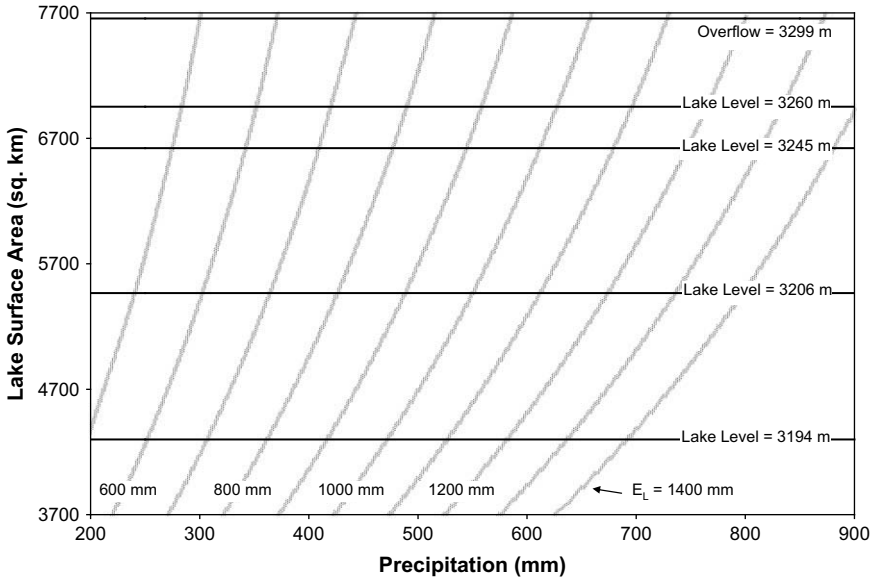

Fig. 6. Equilibrium lake levels in relation to precipitation and evaporation, holding surface inflow coefficient constant ($k = 0.141$). Gray lines represent evaporation values E_L, from 500 mm on left to 1400 mm on right. Lake levels are horizontal lines.

lower alluvial units. Fine-grained aeolian sand fill, taken from one ice/sand wedge cast, returned an OSL age of 22.6 ± 1.8 cal ka (Madsen et al., 2008). If this age estimate is correct, it indicates that the upper alluvium was deposited during a period of renewed alluviation beginning some time after ~22.6 ka (LGM) and before the inception of loess deposition.

Below the alluvial units is a 1.6 m thick layer of well-sorted lacustrine sands (Fig. 11), which in turn lie atop a largely unexposed unit of alluvial gravels. From their base they fine upwards toward the center of unit, coarsening again toward the top. Fine sand laminae occur at the top and bottom of the sequence with ripple laminated fine sand to silt laminae dominant in the middle of the unit. The sand surface has small undulations containing few pebbles and lenses of coarser sand. Two OSL-dated samples from this lacustrine sand unit, one near the base (8 cm above the basal alluvium; UIC2176, Table 1) and another in the middle (80 cm above basal alluvium; UIC2177, Table 1), returned age estimates of 98.9 ± 7.4 and 90.9 ± 6.7 ka, respectively.

A second gravel pit 2.5 km to the east at 3239 m altitude (36.596° N, 100.426° E; Km 2114.5 on the highway) reveals additional nearshore sand deposits and possible calm-water lagoon sediments (Figs. 12, 13). Again, blocky surface Holocene loess ~1.4 m thick tops the section, beneath which is a ~3.7 m thick layer of angular to sub-angular poorly to moderately well-sorted alluvial gravel and cobbles with clasts to 25 cm and occasional fine sand lenses containing scattered small gravel (Fig. 12). A few involutions averaging ~40 cm thick and containing possible aeolian deposits occur in the middle of this unit. At least one soil is apparent in the upper portion of the unit. We obtained a sample of a horizontally bedded coarse sand lens (3.8 m below modern surface) near the base of this bajada alluvium, dated by OSL to $\sim 38.8 \pm 3.0$ ka and $\sim 53.7 \pm 4.0$ ka (Madsen et al., 2008). This date provides confirmation for luminescence ages of ~44.5 and ~45.5 ka on nearby loess lenses within alluvial bajada gravels and ~33.3 and ~16.9 ka on overlying soils reported by Porter et al. (2001), as well as a ^{14}C date of ~43.2 ka on aeolian deposits near the southeastern shoreline (Yuan et al., 1990).

Beneath this alluvial gravel at 4.1–4.28 m depth is a bed of coarse well-sorted sand containing broken mollusc shell, possibly a beach (Fig. 13). Immediately below it is a 2-cm thick band of ripple laminated silty clay that may be lagoon deposits. Underlying these beds are sandy near-shore deposits (4.3–5.0 m depth below surface), consisting of ripple laminated sandy silt at base, coarsening upwards to fine sands. Ripple laminae disappear towards the

Fig. 7. Paleoshorelines and gravel pit east of Haiyin Bay, 3240–3250 m elevation.

Please cite this article in press as: Rhode, D., et al., Paleoenvironmental and archaeological investigations at Qinghai Lake, western China:..., Quaternary International (2009), doi:10.1016/j.quaint.2009.03.004

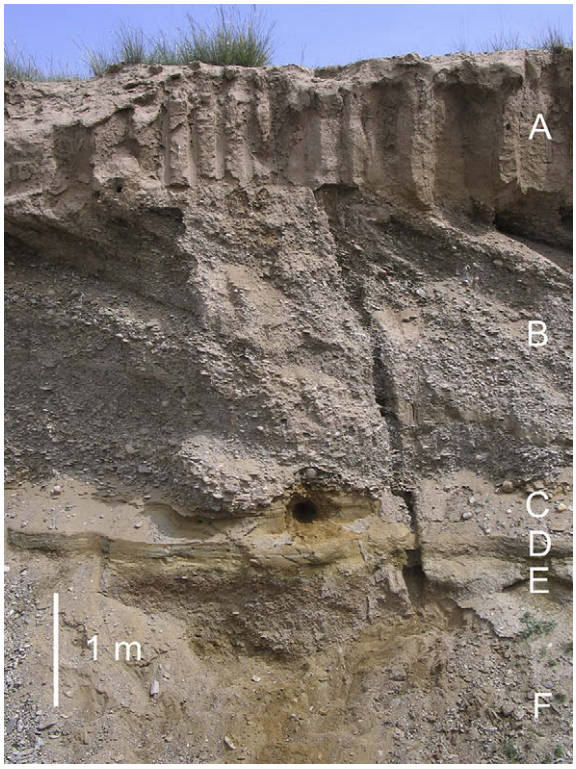

Fig. 8. Gravel pit exposure east of Haiyin Bay, 3240 m elevation. (A) Post-LGM loess. (B) Foreset beach gravels, dipping east. (C) Laminated fine to medium sand. OSL date UIC1829 returned age estimates exceeding ~100 cal ka. (D) Laminated fine sand, silt, and clays with ostracodes and broken shell. Ostracodes yielded an age estimate of ~41 ^{14}C ka, which we regard as effectively infinite and therefore a limiting age. (E) Horizontally bedded sand and small gravel. (F) Angular cobbly alluvium.

top. An OSL sample collected from 20 cm below the top of the unit gave an age estimate of ~93.3 ± 7.1 ka (Madsen et al., 2008). Beneath this ripple laminated sand is a 15 cm thick bed of medium to coarse well sorted sand containing shell fragments (possibly another beach), and below that laminated silty sands at least 20 cm thick but of unknown final depth.

4.4. Jiangxigou

A small perennial stream flows northward out of the Qinghai Nan Shan near the village of Jiangxigou, forming a prominent canyon in the bajada south of Qinghai Lake (Fig. 2). This canyon is notable because it has been subject to several earlier investigations of higher shoreline features (Porter et al., 1991; Wang and Shi, 1992; Nakao et al., 1995a). We conducted archaeological investigations at Upper Paleolithic and Epipaleolithic/Neolithic occupations in the canyon (Madsen et al., 2006; Rhode et al., 2007), and made observations pertinent to paleoenvironmental history as well.

We could find no evidence here of possible shorelines reported to be above 3260 m altitude. A supposed wave-cut platform at ~3330 m elevation is rather the head of a bajada fronting the Qinghai Nan Shan (Porter et al., 2001). Horizontally bedded coarse sand and gravel at this elevation appear to be overland slopewash deposits derived from the head of the canyon here (Nakao et al., 1995a). We obtained two OSL samples of aeolian silty sand filling two separate ice-wedges formed in the alluvium at the highest point of the bajada (Fig. 14) dating to ~45.6 ± 3.4 ka and ~98.4 ± 7.4 ka, respectively (Madsen et al., 2008). An AMS radiocarbon date of ~22.9 cal ka from intrusive organic material also provides a limiting age. Together these age estimates suggest the ice wedges formed before 40 ka, with the top of the fan deposited before 45 ka and possibly before ~98 ka.

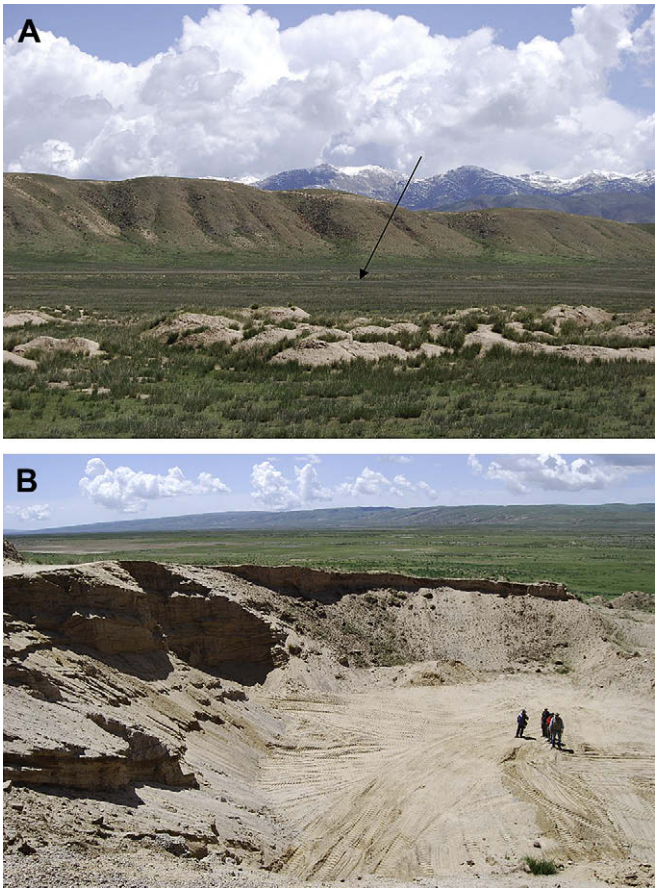

Fig. 9. Paleoshorelines and spit complex, southwestern margin of Riyue Mountains, north of Daotong River. (A) Paleoshoreline at 3260 m at base of bluff (arrow), looking northeast from top of sand spit shown in (B). Note no evidence of shoreline features on exposed bluff in background. Riyue Mountains on far horizon. (B) Exposed section of sandy spit at ~3248 m elevation. Daotong River floodplain is in background.

4.5. Heimahe #1 and #3 archaeological sites

The Heimahe #1 archaeological site (Madsen et al., 2006; Brantingham et al., 2007) is located on the west side of Heimahe Village, in a former borrow pit and present-day sheep corral north of the Heima River, at ~3210 m altitude (36.730° N, 99.771° E; Fig. 2). The exposure consists of 3.5 m of fine sandy silt loess fining upwards to blocky silt loess (Fig. 15). These aeolian deposits overlie fluvial gravels and small cobbles that extend to an unknown depth. Horizontal charcoal stains in the lower third of the exposure indicate brief stable surfaces, at least one of which contains a human occupation site including a hearth, dated by seven ^{14}C dates that average ~13.1 cal ka (Madsen et al., 2006). This archaeological occupation layer is located about 2.11 m below the modern surface. A paleosol occurs at 1.4 m below the surface, above the archaeological occupation. An OSL date from just above the paleosol (134 cm depth) returned a date of ~11.8 ± 0.8 ka (UIC1567, Table 1). This age is consistent with the radiocarbon chronology from the exposure; however, other samples dated by OSL above and below this sample are inconsistent with it or with the radiocarbon chronology (Madsen et al., 2006; Brantingham et al., 2007), so the age of this sample may also be uncertain. The loess is underlain by fluvial sand and gravel, dated by OSL to ~26.5 ± 1.8 ka (UIC1569, Table 1). Zhou et al. (2004) report on geochemical aspects of this section.

Please cite this article in press as: Rhode, D., et al., Paleoenvironmental and archaeological investigations at Qinghai Lake, western China:..., Quaternary International (2009), doi:10.1016/j.quaint.2009.03.004

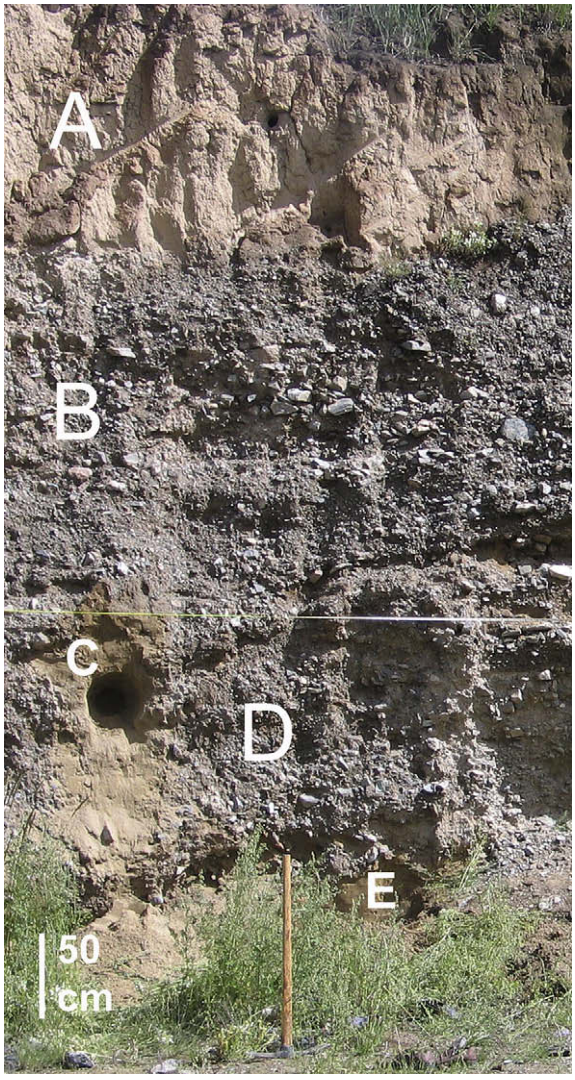

Fig. 10. Gravel pit at KM 2117, 3246 m altitude, bajada south of Qinghai Lake. (A) Post-LGM loess. (B) Upper alluvial fan deposit of angular cobbles and sand. (C) Ground wedge extending down from contact surface at base of upper alluvial fan deposit. This ground wedge returned an OSL date (UIC1652) of ~22.6 cal ka. (D) Lower alluvial deposit of angular cobbles and sand. (E) Fine bedded well-sorted sand, probably lacustrine sand deposit. See Fig. 11.

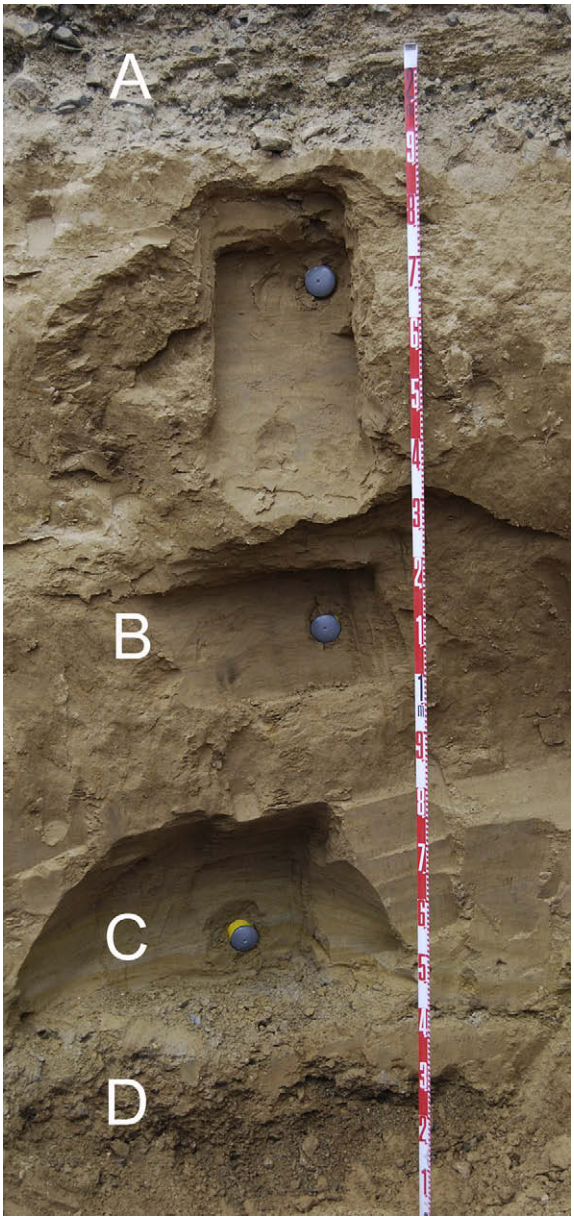

Fig. 11. Lacustrine sand deposit below alluvial materials at gravel pit, KM 2117, 3246 m altitude, bajada south of Qinghai Lake. (A) Alluvial gravels and sands correlative with (D) in Fig. 10. (B) Lacustrine well-sorted fine sand and silt with fine ripple bedding. The OSL age of this sample (UIC2177) is ~90.9 cal ka. (C) Lacustrine well-sorted medium to fine sand. The OSL age of this sample (UIC2176) is ~98.9 cal ka. (D) Underlying alluvial gravels and sands.

The Heimahe #3 archaeological site (Rhode et al., 2007) is a similar stack of fluvial sands and gravels topped by loess, located at ca. 3203 m elevation on the east side of the village on a cutbank of the Heima River (36.724° N, 99.780° E; Fig. 2). At the base of the observed cutbank, 325 cm below the modern surface, is a bed of well-sorted gravels with clasts 2–5 cm in long dimension, and coarse sand filling the interstices (Fig. 16). Above this gravel bed is a 50 cm-thick layer of medium to coarse sands with a few silt lenses inter-fingered. This coarse sand unit is overlain by ripple laminated fine sand fining upward to flat-bedded silty sand, topped by a distinct layer of fine to medium sand with reworked unidentified mollusc shell fragments. The gravel and sand layers likely represent a shoreline interface of stream and lake waters reworked by fluvial or lacustrine action, an incursion of Qinghai Lake to the elevation of this locality. Above this, at 195–230 cm depth, is a layer of sandy silt loess, alternating with flat bedded fine sands, probably aeolian in deposition. The remnant of an archaeological habitation lies within this bed, 195 cm below the modern surface, including a firepit containing poplar (*Populus*) charcoal and a small scatter of artifacts dating to ~8.4 cal ka (Rhode et al., 2007).

The sandy silt loess extends upward to the top of the observed profile. A small sand stringer located at a depth of ca. 170 cm might represent a brief fluvial or lacustrine incursion, but we are uncertain about its derivation. A probable mid-Holocene paleosol is visible at a depth of 115–130 cm below the modern surface. The upper 115 cm of the profile is the modern soil zone, including an organic-rich A horizon of ~20 cm depth, a bioturbated friable weakly prismatic B horizon to 70 cm depth, and a carbonate-rich silt loess beneath that.

4.6. Heimahe road cut

A series of cutbanks occur along the highway northwest of Heimahe Village toward Bird Island, at ~3205–3210 m (+11–16 m)

Please cite this article in press as: Rhode, D., et al., Paleoenvironmental and archaeological investigations at Qinghai Lake, western China:..., Quaternary International (2009), doi:10.1016/j.quaint.2009.03.004

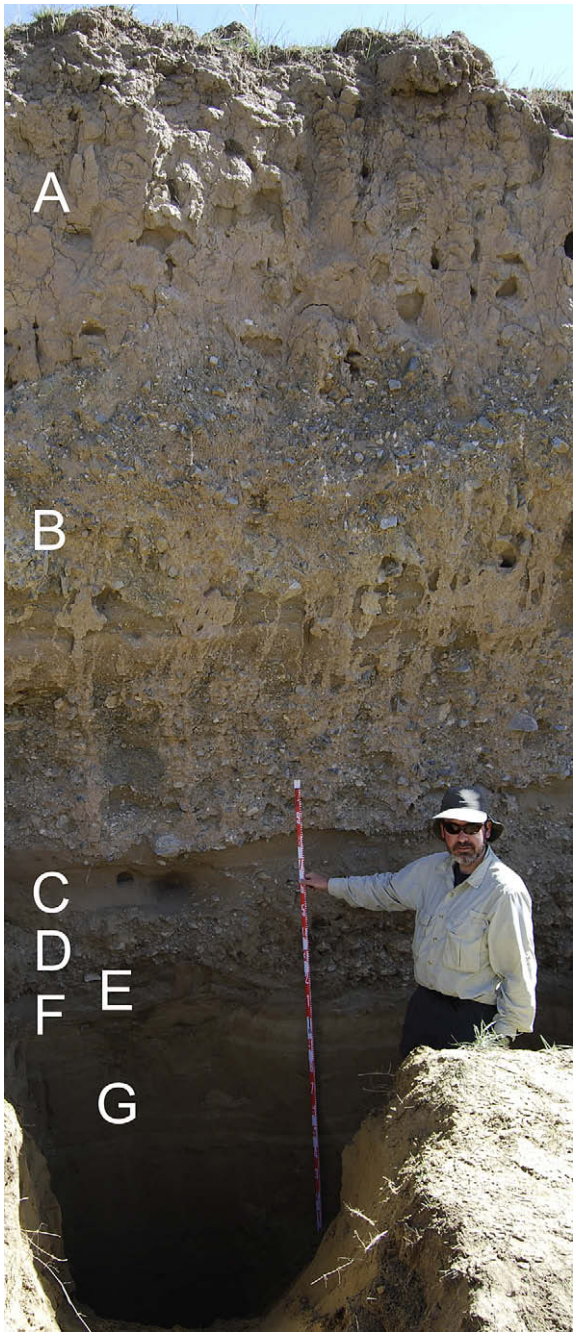

Fig. 12. Exposed deposits at gravel pit, KM 214.5, 3239 m altitude, bajada south of Qinghai Lake. (A) Post-LGM loess. (B) Alluvial gravels and sands, with aeolian lenses. (C) Well-sorted sands, dated by OSL to ~38.8 cal ka (UIC1868gr). (D) Probable alluvial gravel and coarse sand. (E) Coarse well-sorted beach sand containing broken mollusc shell. (F) Thin band of ripple laminated silty clay (lagoon?). (G) Lacustrine ripple laminated sandy silt coarsening upwards to fine sands. An OSL age estimate of a sample 20 cm below the top of this unit yielded a date of ~93.3 cal ka (UIC1828). At ~70 cm below top of unit is a well-sorted coarse sand with broken shell (beach?), and below that ripple laminated silty sands.

on the southwest shore of the lake (36.759° N, 99.771° E; Fig. 2). These reveal a sequence of Holocene and MIS 3 loess units with paleosols, deposited over gravels dating to MIS 5 (Fig. 17).

The uppermost unit consists of late Pleistocene to Holocene loess, ~2.0-2.2 m thick, containing two probable paleosols (at ~1.25–1.45 and ~1.90–2.20 m depth in one exposure). Three OSL age estimates were obtained from this upper loess. One, at the top of the prominent upper paleosol (127 cm depth; UIC1657, Table 1), dates to ~1.5 ± 0.1 ka, indicating that more than a meter of loess has been deposited in places at this site within the past 1500 years. The next sample underlies the upper paleosol but above the lower one (173 cm depth; UIC1656, Table 1), and dates to 12.3 ± 0.9 ka. A third sample, at the base of this upper loess (248 cm depth), dates to ~17.9 ± 1.3 ka (Madsen et al., 2008). This basal date is consistent with previously reported ages for the initiation of loess deposition (Porter et al., 2001).

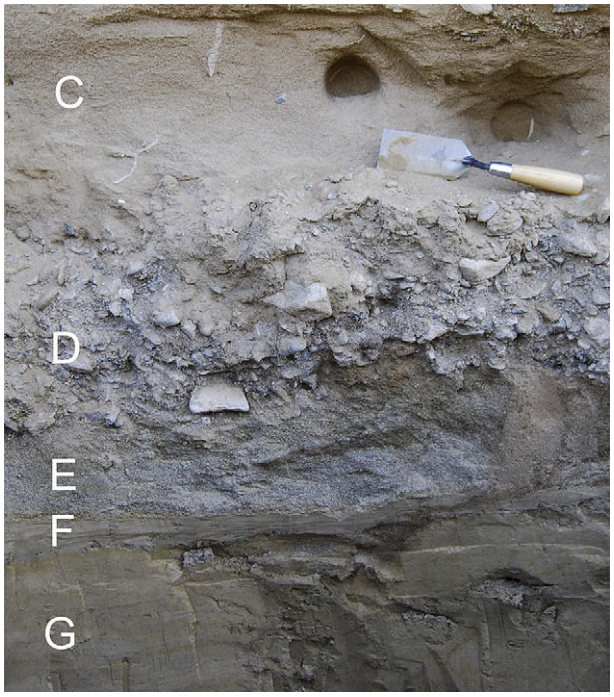

Fig. 13. Close-up of strata C–F as shown in Fig. 12.

This upper loess overlies a distinct unconformity at this locality as well, one on top of a lower sandy silt loess unit. This lower loess fills swales in the underlying gravel unit. The unconformity extends across the top of this lower loess to the level of the high points in the underlying gravel unit, marked by a stone line and a moderately well-developed paleosol remnant. Small ice wedges periodically extend from the unconformity surface into the lower loess, wedges which are filled by sediment from the upper loess above. Sand from this lower sandy loess is dated by OSL to ~25.0 ± 1.9 ka (Madsen et al., 2008).

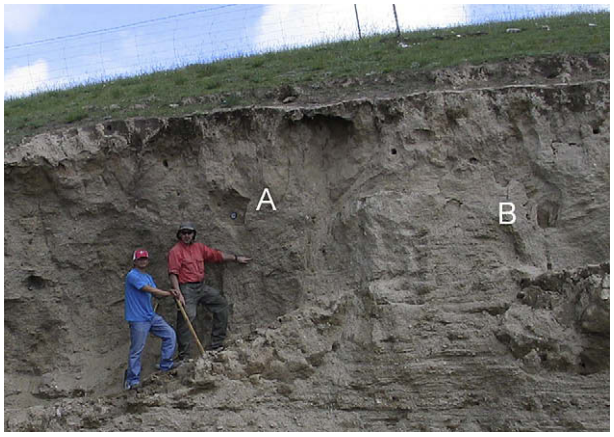

Fig. 14. Alluvial fan deposits at head of Jiangxigou canyon mouth, with two periglacial wedges exposed (A and B). Wedge A returned an OSL age on fine-grained silty sand fill of ~98.4 cal ka (UIC1651).

Please cite this article in press as: Rhode, D., et al., Paleoenvironmental and archaeological investigations at Qinghai Lake, western China:..., Quaternary International (2009), doi:10.1016/j.quaint.2009.03.004

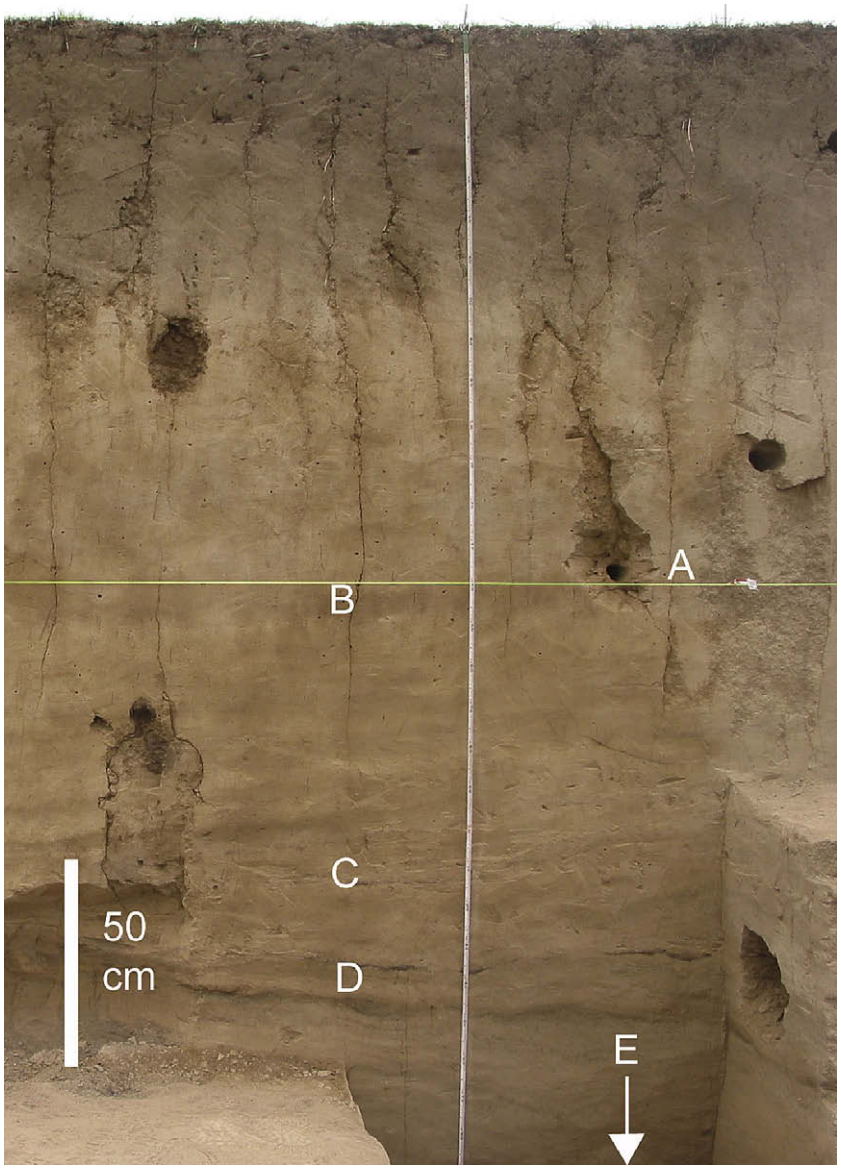

Fig. 15. Stratigraphic profile of Heimahe #1 exposure. (A) OSL sample (UIC1567) yielding an age estimate of ~11.8 cal ka. (B) Faint buried possible paleosol. (C) Depth of buried cultural living floor containing hearth dating to ~13.1 cal ka. (D) Charcoal stained laminae. (E) Fluvial sands and silt blocks ~0.8 m below marker.

The basal unit at this locality consists of sandy gravels and cobbles, the deposit sometimes having a roughly horizontal surface and elsewhere modified to forming rises and swales spaced 2–5 m apart and 0.8–1.0 m deep. The exposure is limited and the gravels may represent either alluvial/fluvial deposits or, more likely, wave-deposited or reworked beach materials. The cobbles are rounded to sub-angular, mostly platy in shape, and moderately well-sorted. The maximum clast size is 5–10 cm diameter. The undersides of the clasts are coated with a stage 2 carbonate layer. They occur in jumbled clasts with a matrix of yellow silt and sand; some unfilled pockets in the jumble are also present, lacking sandy matrix. The gravels are slightly imbricated, dipping gently toward the lake (indicating a possible beach). Erosion into this gravel layer appears to have created the pattern of rises and swales observed in one section. Mantling this gravel layer is a thin band of fine-grained coarsely banded sands and silts, the particles coated with clay skins. On top of this sand and silt layer is an armoring layer of gravels and sands oriented parallel to the surface of the rises and swales. This armor layer appears to be reddened with weathering. The top of the rises is at the same level as the lower sandy loess unit described above; the reddened weathering at the tops of the rises merges with the soil observed on the surface of this lower loess. A sample was collected from a sand lens below the armor layer and above the possible beach gravel in an adjacent road cut, 2.90 m below the surface. It returned two disparate OSL dates depending on method, 94.5 ± 7.1 and 133 ± 10.0 ka (UIC1658Ir and UIC1658Bl, respectively, Table 1; cf. Madsen et al., 2008).

5. Summary of observations

a. Lacustrine geomorphic features and deposits were observed as high as 3260 m altitude (+66 m above modern lake level). Ages of these features as measured by OSL indicate they probably date to late MIS 5 (~75–110 ka). The highest dated feature, a large spit at 3248 m, is dated to ~74 ka. Well-sorted sand deposits interpreted to represent lacustrine and lagoon environments at ~3235–3247 m altitude (+40–53 m above modern lake level), were dated between ~93–105 ka. The highest observed shoreline, at 3260 m, remains undated.

Please cite this article in press as: Rhode, D., et al., Paleoenvironmental and archaeological investigations at Qinghai Lake, western China:..., Quaternary International (2009), doi:10.1016/j.quaint.2009.03.004

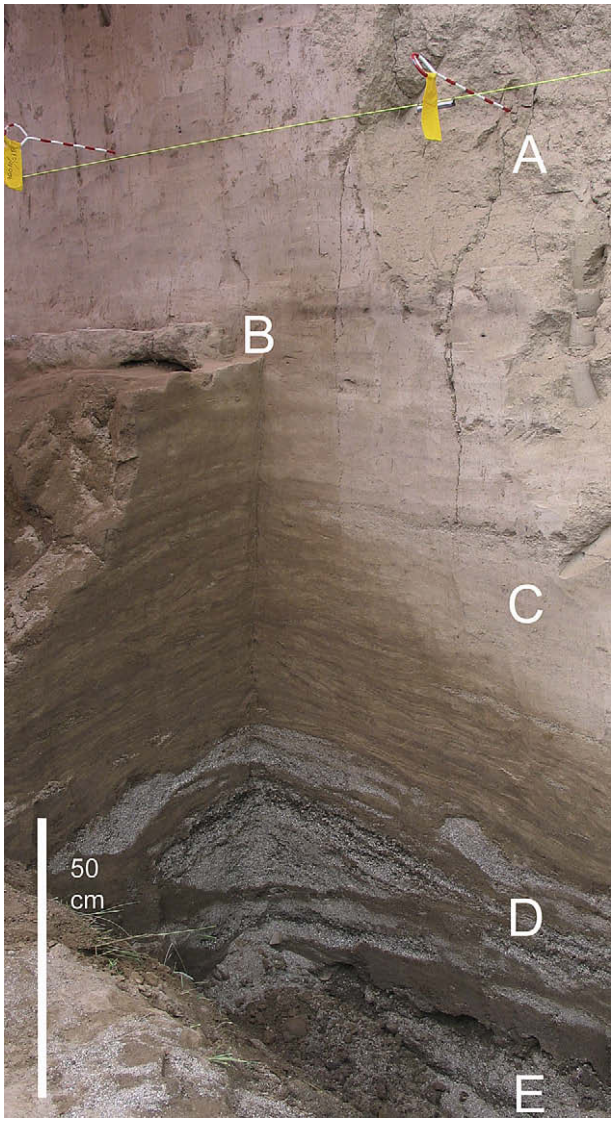

Fig. 16. Stratigraphic profile of lower exposure at Heimahe #3. (A) Holocene loess. (B) Archaeological living surface and firepit, radiocarbon dated to ~8.4 cal ka. (C) Laminated sands and silts with occasional well-sorted medium sand stringers. (D) Medium to coarse sand interspersed with silt blocks. (E) Well-sorted gravel.

b. We saw no evidence of suggested lake deposits and shorelines located above 3260 m. Several reported features thought to be paleoshorelines at higher elevations appear to be alluvial deposits (Nakao et al., 1995a; Porter et al., 2001).
c. No MIS 3 lake deposits were observed, though such evidence may have been removed or obscured by widespread regional erosion that occurred prior to or during the LGM, or hidden by subsequent deposition of post-LGM loess. Evidence from alluvial sequences as well as core data from the lake itself suggests relatively modest lake elevations during last ~40 ka, often beneath the level of the present lake (Yu, 2005).
d. Many alluvial deposits in the lower basin were laid down during MIS 3 (Porter et al., 2001; Owen et al., 2006). Many of these deposits also show evidence of extensive erosion and unconformities, often in association with periglacial features. This widespread erosion likely occurred just before and possibly during a cold and dry LGM.
e. Post-LGM loess began to be deposited by ~16–18 ka, confirming the chronology reported by Porter et al. (2001). It is earlier than that reported by Küster et al. (2006) for the Qilian Mountains north of Qinghai Lake Basin. We recognized two paleosols in this loess, one of pre-Younger Dryas age dating to before ~12.3 ka and a second that is probably middle Holocene in age. The younger paleosol may be related to a mid-Holocene soil on the lake's south shore containing spruce (*Picea*) charcoal dating to ~4.6 ka (Kaiser et al., 2007). Kaiser et al. also identified an older paleosol whose age is constrained by a date of ~9.2 ka on spruce charcoal from the base of colluvium overlying the paleosol.

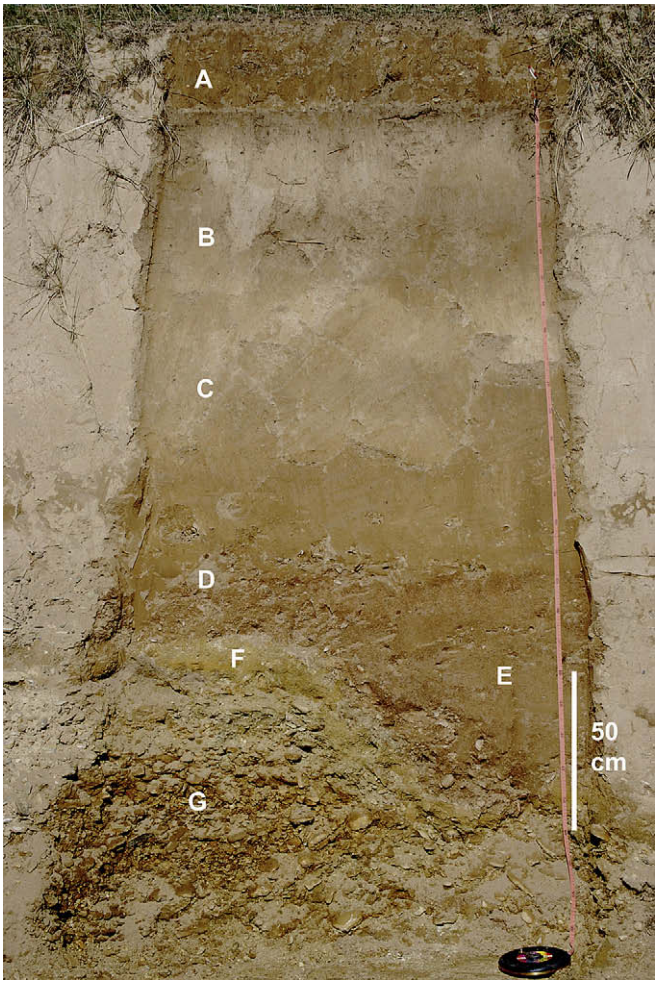

Fig. 17. Heimahe road cut profile. (A) Modern surface soil. (B) Buried paleosol in post-LGM loess. An OSL sample from just above this soil yielded an age estimate of ~1.5 cal ka (UIC1657). (C) Probable lower paleosol within loess. An OSL sample between B and C yielded an age of ~12.3 cal ka (UIC1656); an OSL sample in loess below this unit but above D yielded an age estimate of ~17.9 cal ka (UIC1659). (D) Weathered surface (remnant paleosol) and stone line dividing upper post-LGM loess (A, B, C) from lower pre-LGM sand/loess (E) This surface occasionally contains periglacial wedges filled with loess from above. (E) Pre-LGM sandy loess, filling swales left in underlying sands and gravels (F, G). An OSL sample from this lower loess yielded an age estimate of ~25.0 cal ka (UIC1830). (F) Armoring weathered layer of gravels and sands oriented parallel to the surface of the rises and swales, underlain by fine-grained coarsely banded sands and silts, the particles coated with clay skins. An OSL sample from this unit yielded two disparate dates, ~94.5 and ~133.0 cal ka (UIC1658). (G) Jumbled sandy gravels and cobbles occurring in a series of low ridges and swales.

6. Discussion

The lake highstands above 3230 m imply a hydrologic balance dramatically different than the one that exists today in the Qinghai Lake Basin, a hydrologic balance that may not have existed for the

Please cite this article in press as: Rhode, D., et al., Paleoenvironmental and archaeological investigations at Qinghai Lake, western China:..., Quaternary International (2009), doi:10.1016/j.quaint.2009.03.004

past 70,000 years. As noted in Table 3, a lake with a surface altitude of 3260 m would occupy a surface area of ~6952 km^2, about 1.6 times that of the modern. Maintenance of a lake at this level would require a significantly greater ratio of precipitation over evaporation, and/or greater runoff generated from precipitation, to reach equilibrium. What amount of precipitation and runoff would be needed to offset evaporation, sufficient to support a lake at 3260 m altitude? Water balance modeling of Qinghai Lake shows that precipitation, runoff, and evaporation all are critical to lake level changes (Qin, 1994, 1997; Nakao et al., 1995b; Qin and Huang, 1998; Yan et al., 2002; Li et al., 2007). The water balance model used here indicates that to maintain a lake at the 3260 m level would require annual average precipitation of ~550 mm (~1.4–1.6 times modern estimates) or a decrease in evaporation to ~650 mm (a reduction of 30–40% below modern), or some similar combination assuming that runoff generation was close to modern values (Fig. 6). This is consistent with previous water balance modeling at Qinghai Lake (Qin, 1994, 1997; Qin and Huang, 1998; Jia et al., 2000; cf. Colman et al., 2007).

If the high lakes do prove to be MIS 5 and not later, several obvious questions are raised. What factors caused the high lakes? And, what conditions have changed so that high lakes no longer occur? Although we cannot provide answers to these questions, we can speculate on a range of possible causes.

First, the East Asian monsoon may have been significantly stronger during MIS 5, bringing more precipitation to the northeast Qinghai–Tibet Plateau than during the later MIS 3 and Holocene monsoon peaks (cf. Porter et al., 1992; Shi et al., 1999; Yang et al., 2004; Yuan et al., 2004; Wang et al., 2005). A strong East Asian Monsoon, developed during intervals of high summer insolation at ~75–85 (MIS 5a) and ~105 ka (MIS 5c), is recorded in speleothem records (Wang et al., 2001; Yuan et al., 2004; Li et al., 2005; Johnson et al., 2006; Kelly et al., 2006), particularly at ~107 ka and between ~86–80 ka, and in the Chinese loess record (An et al., 1991; Chen et al., 1999; Porter, 2001; Lu et al., 2004, 2006, 2007; Guan et al., 2007). The central Chinese loess record suggests that the winter westerlies system was weaker during MIS 5, so that the East Asian summer monsoon frontal position pushed further northward (Chen et al., 1990; Ding et al., 1995). The East Asian summer monsoon does not appear to have been exceptionally strong during MIS 3, so a lack of significant Qinghai Lake highstands during this period is to be expected (Colman et al., 2007). Possibly the East Asian monsoon was weaker during MIS 3 and after the LGM as a result of lower sea level, exposing the Sunda Shelf (An et al., 1991; Tamburini et al., 2003). The East Asian summer monsoon appears to have reached a peak of strength in northwest China during the early Holocene summer insolation peak (An et al., 2000; He et al., 2004), but that peak may have been less strong than during MIS 5, again possibly because sea level had not risen fully by the early Holocene, whereas the ocean level was high during MIS 5.

A second possible cause of the difference between the period of large lakes and the subsequent modest-lake period may have to do with the effects of evaporation from the lake and its basin. Evaporation obviously has a strong effect on water balance and consequently lake level, but it is a complex function of solar radiation intensity, cloudiness, wind speed, humidity, air temperature, water surface temperature, albedo, and ice cover. Modeling conducted by Qin and Huang (1998) shows that proportional changes in precipitation have the greatest effect on lake level, changes in cloudiness affecting evaporation have a smaller effect, and changes in air temperature has a smaller effect still. Qin and Huang's results indicate that a one-degree change in mean annual temperature alone would yield a ~8.5% shift in runoff, a ~8% change in evaporation, and consequently a ~80–90 mm change in lake level per year.

Porter et al. (1992) provide global circulation model estimates suggesting that MIS 5 (126 ka) summer precipitation may have been ~3 mm/day greater, summer temperature ~2.5 °C greater, and winter temperature ~2.5 °C less than today. Feng et al. (1998) give similar estimates for the western Chinese Loess Plateau. If these values are reasonable, and following the estimates by Qin and Huang, then during MIS 5 the temperature increase would have raised summer evaporation by ~25%, but summer precipitation would have roughly doubled, more than offsetting the evaporation change.

By way of contrast, the modeled values for the strong early Holocene monsoon peak (An et al., 2000; He et al., 2004) is a ~2.5 mm/day increase in summer precipitation and ~1 °C increase in summer temperature, compared with today. These values suggest that precipitation may have increased ~250 mm more than today, while evaporation may have been only about 8% more than today. These values are not much less than the modeled MIS 5 conditions, and under such circumstances a large early Holocene lake level rise might be expected. But, as discussed, we and others (Lister et al., 1991; Yu, 2005) see no evidence for it in the Qinghai Lake record.

A third possible cause of the difference could be that the proportion of runoff generated from precipitation might have been greater. If the proportion of inflow into Qinghai Lake relative to precipitation at the lake can be used as a rough gauge, then the amount of inflow presently generated per unit area of the Qinghai Lake Basin (less the area of the lake) is ~0.141 times the amount of precipitation falling on a unit area of Qinghai Lake itself. If this proportion were to increase, to 0.2 or 0.3, the amount of additional inflow would be dramatically higher (Fig. 5). There is no reason to suppose, however, that basin runoff conditions during late MIS 5 were especially different than during MIS 3 or today. We might expect runoff generation to be greatest during periods when much of the basin was largely unvegetated, sealed in permafrost or undergoing heavy erosion, as during the LGM. Yet because precipitation was also apparently quite diminished during the LGM when these conditions applied, the lake level was also correspondingly very low. Modern human land use practices may also increase runoff, a factor which would not have existed during MIS 5, MIS 3, or the LGM. At present we do not know what surface conditions might have prevailed during MIS 5 that would increase the proportion of runoff generated. Given the sensitivity of lake area to small changes in runoff generation, this possible factor cannot be dismissed.

Fourth, precipitation brought to the region by prevailing westerlies may have been a stronger contributing factor than at present. Lakes in extreme western China often are influenced more strongly by westerly-derived precipitation than by summer monsoonal precipitation (Yang et al., 2004, 2006). Chen et al. (2008) suggest that westerly moisture flow affects arid central Asia more so than does the East Asian monsoon, and that the two sources of precipitation are out of phase temporally. Could a stronger westerly-dominated precipitation regime during MIS 5 have raised Qinghai Lake to higher levels? This possibility seems doubtful. While Qinghai Lake is at the crossroads of both the Atlantic westerlies and the Asian monsoons, the moist East Asian summer monsoon system tends to dominate in interglacial periods (such as MIS 5) while the drier westerlies dominate in glacial periods (Vandenberghe et al., 2006), and the Qinghai record fits more with the East Asian monsoon model than the westerly model. Winter westerlies at Xining, east of Qinghai Lake, appear to have been weaker during MIS 5 than during the Holocene, not stronger (Lu et al., 2006; Vandenberghe et al., 2006), which supports the idea that East Asian monsoons fed the high levels of Qinghai Lake. Large lakes were supported in the Tengger Desert in arid Central Asia during MIS 3

Please cite this article in press as: Rhode, D., et al., Paleoenvironmental and archaeological investigations at Qinghai Lake, western China:..., Quaternary International (2009), doi:10.1016/j.quaint.2009.03.004

(Zhang et al., 2004a), presumably as a result of enhanced westerly-derived precipitation, but large lakes do not appear to have been supported in the Qinghai Lake Basin. However, strengthened westerlies during MIS 3 may help explain why monsoons were not a strong force for the generation of large lakes in the Qinghai Lake Basin (Fang et al., 1999; Colman et al., 2007).

A fifth scenario concerns watershed modification and drainage capture. This region is tectonically very active, and stream capture is an important component of landscape evolution (Li et al., 1997, 2000; Li and Fang, 1999; Lehmkuhl and Haselein, 2000; Fang et al., 2005; Harkins et al., 2007). Qinghai Lake itself owes its present closed-basin status to tectonic uplift of the divide between it and the headwaters of the Yellow River (Pan, 1994; Li et al., 1996). The period around 100–150 ka BP appears to have been especially active on a landscape modifying scale (Li et al., 2000; Zhang et al., 2004b; Su et al., 2005). If the size of the watershed that fed Qinghai Lake was reduced after ~70 ka by tectonically driven stream capture, this landscape process could explain the lack of high lake stands after that time without invoking a post-MIS 5 reduction in the strength of the East Asian monsoon.

We turn now to an issue that initiated our investigations, the archaeological record of human occupation of the Qinghai Lake Basin during the late Pleistocene. As we have noted, well-dated evidence of human occupation of this region extends back to ~15 ka but no earlier. Where might we expect to find earlier records of human habitation, if such records exist?

Our observations suggest that such records, if they predate the age of post-LGM loess deposition, are not likely to have been preserved and will be exceedingly difficult to find. Most of the gently sloping lower lake basin, where human occupation is most likely, is now covered in post-LGM loess and therefore obscured. A cold and dry LGM environment would have been extremely unfavorable for human habitation of the Qinghai Lake Basin. Widespread regional erosion in the basin prior to the LGM would have hindered preservation of earlier human occupation on the piedmonts and slopes. Earlier loess deposits such as those found at the Heimahe road cut (that could possibly contain evidence of pre-LGM human occupation) appear to be quite rare. The extensive alluviation during MIS 3 may have buried archaeological sites toward the toes of alluvial fans near the lake margin (cf. Owen et al., 2006). However, during MIS 3 the lake may have been significantly lower, and those buried sites may now be underwater and 4–6 km offshore (Yu, 2005). In sum, our present understanding of landscape evolution in the Qinghai Lake Basin suggests that if people lived in the region during the pre-LGM period, the archaeological record of their occupation will be difficult to detect, apart from a few isolated artifacts.

7. Conclusions

Based on observations accumulated over the past several field seasons, we have suggested a revised late Pleistocene Qinghai Lake shoreline history (Madsen et al., 2008). We observed no significant late Pleistocene highstand features higher than ~3260 m. Shoreline features and deposits between ~3220–3260 m altitude appear to date to late MIS 5, and probably include multiple highstands. A transgressive lake at 3240 m that may have eventually reached at least as high as ~3247 m is dated to ~110–90 ka (late MIS 5c). Another highstand is recorded in the large spit complex at 3248 m, dating to ~75 ka (latest MIS 5a).

We found no evidence of high shorelines above ~3230 m that post-date ~70 ka. Evidence suggesting that Qinghai Lake stood at relatively low intervals after 70 ka include alluvium dating to ~45–18 ka that is unmarked by shoreline development, core data suggesting low lake elevations after ~35 ka and possibly after ~70 ka (Yu, 2005), and the absence of lake deposits in low-elevation exposures dating ~95–25 ka (e.g., the Heimahe road cut). These observations suggest that lake level rises during MIS 3, late glacial termination, and the Holocene climatic optimum were modest compared to earlier lake highstands.

The Qinghai Lake shoreline record requires much additional age control and refinement, but it has strong potential to contribute to our understanding of the timing, strength, and distribution of late MIS 5 monsoon systems, of the relation of monsoons to continental Westerly climatic regimes (Vandenberghe et al., 2006), of the role of the Qinghai–Tibet Plateau as an amplifier of regional climatic systems (An et al., 2001; Liu and Yin, 2002; Liu et al., 2003; Harris, 2006), of late Pleistocene tectonic controls and the role of stream capture in landscape development in the northeastern Plateau, and of early human occupation of the Tibetan high country.

Acknowledgments

Support for this research came from the US National Science Foundation (INT-0214870), the Desert Research Institute, the University of California Los Angeles, the University of Arizona, the Mercyhurst Archaeological Institute, the University of Texas, the Santa Fe Institute, the Wenner-Gren Foundation, USA, and by the Qinghai Institute of Salt Lakes, Chinese Academy of Sciences, PRC.

References

Aitken, M.J., Bowman, S.G.E., 1975. Thermoluminescent dating: Assessment of alpha particle contribution. Archaeometry 17, 132–138.
Aldenderfer, M.S., 2003. Moving up in the world: Archaeologists seek to understand how and when people came to occupy the Andean and Tibetan plateaus. American Scientist 91, 542–550.
Aldenderfer, M.S., 2006. Modelling plateau peoples: The early human use of the world's high plateaux. World Archaeology 38, 357–370.
An, Z., Kukla, G.J., Porter, S.C., Jule, X., 1991. Magnetic susceptibility evidence of monsoon variation on the Loess Plateau of central China during the last 130,000 years. Quaternary Research 36, 29–36.
An, Z.S., Porter, S.C., Kutzbach, J.E., Wu, X.H., Wang, S.M., Liu, X.D., Li, X.Q., Zhou, W.J., 2000. Asynchronous Holocene optimum of the East Asian monsoon. Quaternary Science Reviews 19, 734–762.
An, Z., Kutzbach, J.E., Prell, W.L., Porter, S.C., 2001. Evolution of Asian monsoons and phased uplift of the Himalaya-Tibetan plateau since Late Miocene times. Nature 411, 62–66.
Balescu, S., Lamothe, M., 1992. The blue emission of K-feldspar coarse grains and its potential for overcoming TL age. Quaternary Science Reviews 11, 45–51.
Benn, D.I., Owen, L.A., 1998. The role of the Indian summer monsoon and the mid-latitude westerlies in Himalayan glaciation: review and speculative discussion. Journal of the Geological Society 155, 353–363.
Brantingham, P., Gao, X., 2006. Peopling of the northern Tibetan Plateau. World Archaeology 38, 387–414.
Brantingham, P.J., Gao, X., Olsen, J.W., Ma, H., Rhode, D., Zhang, H., Madsen, D.B., 2007. A short chronology for the peopling of the Tibetan Plateau. In: Madsen, D.B., Chen, F.H., Gao, X. (Eds.), Late Quaternary Climate Change and Human Adaptation in Arid China. Developments in Quaternary Science, 9. Elsevier, Amsterdam, pp. 129–150.
Brantingham, P.J., Ma, H., Olsen, J.W., Gao, X., Madsen, D.B., Rhode, D., 2003. Speculation on the timing and nature of Late Pleistocene hunter-gatherer colonization of the Tibetan Plateau. Chinese Science Bulletin 48, 1510–1516.
Chen, K.Z., Bowler, J.M., Kelts, K., 1990. Paleoclimatic evolution within the Qinghai-Xizang (Tibet) Plateau in the last 40,000 years. Quaternary Science 1, 21–31 (in Chinese).
Chen, F.H., Bloemendal, J., Feng, Z.D., Wang, J.M., Parker, E., Guo, Z.T., 1999. East Asian monsoon variations during Oxygen Isotope Stage 5: evidence from the northwestern margin of the Chinese loess plateau. Quaternary Science Reviews 18, 1127–1135.
Chen, F., Yu, Z., Yang, M., Ito, E., Wang, S., Madsen, D.B., Huang, X., Yan, Z., Sato, T., Birks, H.J.B., Boomer, I., Chen, J., An, C., Wünnemann, B., 2008. Holocene moisture evolution in arid central Asia and its out-of-phase relationship with Asian monsoon history 27, 351–364.
Colman, S.M., Yu, S., An, Z., Shen, J., Henderson, A.C.G., 2007. Late Cenozoic climate changes in China's western interior: a review of research on Lake Qinghai and comparison with other records. Quaternary Science Reviews 26 (17–18), 2281–2300.

Ding, Z., Liu, T., Rutter, N.W., Yu, Z., Guo, Z., Zhu, R., 1995. Ice-volume forcing of east Asian winter monsoon variations in the past 800,000 years. Quaternary Research 44, 149–159.

Fang, X., Ono, Y., Fukusawa, H., Pan, B., Li, J., Guan, D., Oi, K., Tsukamoto, S., Torii, M., Mishima, T., 1999. Asian summer monsoon instability during the past 60,000 years: magnetic susceptibility and pedogenic evidence from the western Chinese Loess Plateau. Earth and Planetary Science Letters 168, 219–232.

Fang, X., Yan, M., Van der Voo, R., Rea, D.K., Song, C., Parés, J.M., Gao, J., Nie, J., Dai, S., 2005. Late Cenozoic deformation and uplift of the NE Tibetan Plateau: Evidence from high-resolution magnetostratigraphy of the Guide Basin, Qinghai Province, China. GSA Bulletin 117, 1208–1225.

Feng, Z.D., Chen, F.H., Tang, L.Y., Kang, J.C., 1998. East Asian monsoon climates and Gobi dynamics in marine isotope stages 4 and 3. Catena 33, 29–46.

Forman, S.L., Pierson, J., 2002. Late Pleistocene luminescence chronology of loess deposition in the Missouri and Mississippi river valleys, United States. Palaeogeography, Palaeoclimatology, Palaeoecology 186, 25–46.

Guan, Q., Pan, B., Gao, H., Li, B., Wang, J., Su, H., 2007. Instability characteristics of the East Asian Monsoon recorded by high-resolution loess sections from the last interglacial (MIS5). Science in China Series D: Earth Sciences 50, 1067–1075.

Harkins, N., Kirby, E., Heimsath, A., Robinson, R., Reiser, U., 2007. Transient fluvial incision in the headwaters of the Yellow River, northeastern Tibet, China. Journal of Geophysical Research 112.

Harris, N., 2006. The elevation history of the Tibetan Plateau and its implications for the Asian monsoon. Palaeogeography, Palaeoclimatology, Palaeoecology 241, 4–15.

He, Y., Theakestone, W.H., Zhang, Z.L., Zhang, D., Yao, T.D., Chen, T., Shen, Y.P., Pang, H.X., 2004. Asynchronous Holocene climatic change across China. Quaternary Research 61, 60–61.

Henderson, A.C.G., Holmes, J.A., Zhang, J., Leng, M.J., Carvalho, L.R., 2003. A carbon- and oxygen-isotope record of recent environmental change from Qinghai Lake, NE Tibetan Plateau. Chinese Science Bulletin 48, 1463–1468.

Herzschuh, U., 2006. Palaeo-moisture evolution at the margins of the Asian monsoon during the last 50 ka. Quaternary Science Reviews 25, 163–178.

Herzschuh, U., Kürschner, H., Mischke, S., 2006. Temperature variability and vertical vegetation belt shifts during the last ~50,000 yr in the Qilian Mountains (NE margin of the Tibetan Plateau, China). Quaternary Research 66, 133–146.

Huang, W., 1994. The prehistoric human occupation of the Qinghai-Xizang plateau. Götinger Geographische Abhandlungen 95, 201–219.

Huang, W., Hou, Y., 1998. A perspective on the archaeology of the Pleistocene-Holocene transition in north China and the Qinghai–Tibetan Plateau. Quaternary International 49/50, 117–127.

Jain, M., Botter-Jensen, L., Singhvi, A.K., 2003. Dose evaluation using multiple-aliquot quartz OSL: test of methods and a new protocol for improved accuracy and precision. Radiation Measurements 37, 67–80.

Ji, J., Shen, J., Balsam, W., Chen, J., Liu, L., Liu, X., 2005. Asian monsoon oscillations in the northeastern Qinghai–Tibet Plateau since the late glacial as interpreted from visible reflectance of Qinghai Lake sediments. Earth and Planetary Science Letters 233, 61–70.

Jia, Y.L., Shi, Y.F., Fan, Y.Q., 2000. Water balance of paleolake Qinghai and its precipitation estimation at three high lake-level stages since 40 ka BP. Journal of Lake Sciences 12, 211–218 (in Chinese, with English abstract).

Johnson, K.R., Ingram, B.L., Sharp, W.D., Zhang, P., 2006. East Asian summer monsoon variability during Marine Isotope Stage 5 based on speleothem $\delta^{18}O$ records from Wanxiang Cave, central China. Palaeogeography, Palaeoclimatology, Palaeoecology 236, 5–19.

Kaiser, K., Schoch, W.H., Miehe, G., 2007. Holocene paleosols and colluvial sediments in Northeast Tibet (Qinghai Province, China): Properties, dating and paleoenvironmental implications. Catena 69, 91–102.

Kelly, M.J., Edwards, R.L., Cheng, H., Yuan, D., Cai, Y., Zhang, M., Lin, Y., An, Z., 2006. High resolution characterization of the Asian Monsoon between 146,000 and 99,000 years B.P. from Dongge Cave, China and global correlation of events surrounding Termination II. Palaeogeography, Palaeoclimatology, Palaeoecology 236, 20–38.

Kelts, K., Chen, K.Z., Lister, G.S., Yu, J.Q., Gao, Z., Neissen, F., Bonani, G., 1989. Geological fingerprints of climate history—a cooperative study of Qinghai Lake, China. Eclogae Geologica Helvetica 82, 167–182.

Küster, Y., Hetzelb, R., Krbetschek, M., Tao, M., 2006. Holocene loess sedimentation along the Qilian Shan (China): significance for understanding the processes and timing of loess deposition. Quaternary Science Reviews 25, 114–125.

Lang, A., Hatte, C., Rousseau, D.-D., Antoine, P., Fontugne, M., Zoller, L., Hambach, U.A., 2003. High-resolution chronologies for loess: comparing AMS ^{14}C and optical dating results. Quaternary Science Reviews 22, 953–959.

Lanzhou Institute of Geology, 1979. Qinghai Lake Monograph 1961 Expedition. Science Press Series, Beijing (in Chinese).

Lehmkuhl, F., Haselein, F., 2000. Quaternary paleoenvironmental change on the Tibetan Plateau and adjacent areas (western China and western Mongolia). Quaternary International 65/66, 121–146.

Li, J.J., Fang, X.M., 1999. Uplift of Qinghai–Tibetan plateau and environmental change. Chinese Science Bulletin 44, 2217–2224.

Li, J., Fang, X., Ma, H., Zhu, J., Pan, B., Chen, H., 1996. Geomorphological and environmental evolution of the Yellow River during the late Cenozoic. Science in China (Series D) 39, 380–390.

Li, J.J., Fang, X.M., Van der Voo, R., Zhu, J.J., Niocaill, C.M., Ono, Y., Pan, B.T., Zhong, W., Wang, J.L., Sasaki, T., Zhang, Y.T., Cao, J.X., Kang, S.C., Wang, J.M., 1997. Magnetostratigraphic dating of river terraces: rapid and intermittent incision by the Yellow River of the northeastern margin of the Tibetan Plateau during the Quaternary. Journal of Geophysical Research 105, 10121–10132.

Li, C., Yin, H., Yu, Q., 2000. Evolution of drainage systems and its developing trend in connection with tectonic uplift of eastern Kunlun Mt. Chinese Science Bulletin 45, 1904–1908.

Li, H.C., Ku, T.L., You, C.F., Cheng, H., Edwards, R.L., Ma, Z.B., Tsai, W.S., Li, M.D., 2005. $^{87}Sr/^{86}Sr$ and Sr/Ca in speleothems for paleoclimatic reconstruction in central China between 70 and 280 kyr ago. Geochimica et Cosmochimica Acta 69, 3933–3947.

Li, X.Y., Xu, H.Y., Sun, Y.L., Zhang, D.S., Yang, Z.P., 2007. Lake-level change and water balance analysis at Lake Qinghai, west China during recent decades. Water Resources Management 21, 1505–1516.

Lister, G.S., Kelts, K., Chen, K.Z., Yu, J.Q., Neissen, F., 1991. Lake Qinghai, China: closed-basin lake levels and the oxygen isotope record for ostracoda since the latest Pleistocene. Palaeogeography, Palaeoclimatology, Palaeoecology 84, 141–162.

Liu, X., Yin, Z.Y., 2002. Sensitivity of East Asian monsoon climate to the uplift of the Tibetan Plateau. Palaeogeography, Palaeoclimatology, Palaeoecology 183, 223–245.

Liu, X., Shen, J., Wang, S., Yang, X., Tong, G., Zhang, E., 2002. A 16,000-year pollen record of Qinghai Lake and its paleoclimate and palaeoenvironment. Chinese Science Bulletin 47, 1931–1936.

Liu, X.D., Kutzbach, J.E., Liu, Z., An, Z., Li, L., 2003. The Tibetan Plateau as amplifier of orbital-scale variability of the East Asian monsoon. Geophysical Research Letters 30, 1839.

Lu, H., Wang, X., Ma, H., Tan, H., Vandenberghe, J., Mial, X., Li, Z., Sun, Y., An, Z., Cao, G., 2004. The Plateau Monsoon variation during the past 130 kyr revealed by loess deposit at northeast Qinghai–Tibet (China). Global and Planetary Change 41, 207–214.

Lu, H., Vandenberghe, J., Miao, X., Tan, H., Ma, H., 2006. Evidence for an abrupt climatic reversal during the Last Interglacial on the northeast Qinghai–Tibetan Plateau. Quaternary International 154–155, 136–140.

Lu, Y.C., Wang, X.L., Wintle, A.G., 2007. A new OSL chronology for dust accumulation in the last 130,000 yr for the Chinese Loess Plateau. Quaternary Research 67, 152–160.

LZBCAS (Lanzhou Branch of Chinese Academy of Science), 1994. Evolution of recent environment of Qinghai Lake and its prediction. West Center of Resource and Environment, Chinese Academy of Sciences. Science Press, Beijing (in Chinese).

Madsen, D.B., Ma, H., Brantingham, P.J., Gao, X., Rhode, D., Zhang, H., Olsen, J.W., 2006. The late Upper Paleolithic occupation of the northern Tibetan Plateau margin. Journal of Archaeological Science 33, 1433–1444.

Madsen, D.B., Chen, F.H., Gao, X. (Eds.), 2007. Late Quaternary Climate Change and Human Adaptation in Arid China. Developments in Quaternary Science, 9. Elsevier, Amsterdam.

Madsen, D.B., Ma, H., Rhode, D., Brantingham, P.J., Forman, S.L., 2008. Age constraints on the late Quaternary evolution of Qinghai Lake, Tibetan Plateau. Quaternary Research 69, 316–325.

Métivier, F., Gaudermer, Y., Tapponnier, P., Meyer, B., 1998. Northeastward growth of the Tibetan Plateau deduced from balanced reconstruction of two depositional areas: The Qaidam and Hexi Corridor basins, China. Tectonics 17, 823–842.

Nakao, K., Tanoue, R., Okayama, M., 1995a. Geomorphological history of the Basin and the origin of Qinghai Lake, Qinghai Plateau, China. Journal of the Faculty of Science, Hokkaido University, Series VII (Geophysics) 9, 509–523.

Nakao, K., Urakami, K., Momoki, Y., 1995b. Paleohydrologiccal evaluations for Qinghai Lake, Qinghai Plateau, China, on the climatic changes since the late Pleistocene. Journal of the Faculty of Science, Hokkaido University, Series VII (Geophysics) 9, 525–539.

Owen, L.A., Finkel, R.C., Ma, H., Barnard, P.L., 2006. Late Quaternary landscape evolution in the Kunlun Mountains and Qaidam Basin, northern Tibet: A framework for examining the links between glaciation, lake level changes and alluvial fan formation. Quaternary International 154–155, 73–86.

Pan, B., 1994. Research upon the geomorphologic evolution of the Guide Basin and the development of the Yellow River. Arid Land Geography 7, 43–50 (in Chinese).

Porter, S.C., 2001. Chinese loess record of monsoon climate during the last glacial-interglacial cycle. Earth-Science Reviews 54, 115–128.

Porter, S.C., An, Z., Zheng, H., 1992. Cyclic Quaternary alluviation and terracing in a nonglaciated drainage basin on the north flank of the Qinling Shan, central China. Quaternary Research 38, 157–169.

Porter, S.C., Singhvi, A., An, Z., Lai, Z., 2001. Luminescence age and palaeoenvironmental implications of a late Pleistocene ground wedge on the northeastern Tibetan Plateau. Permafrost and Periglacial Processes 12, 203–210.

Prescott, J.R., Hutton, J.T., 1994. Cosmic ray contributions to dose rates for luminescence and ESR dating: large depths and long-term time variations. Radiation Measurements 23, 497–500.

Qin, B., 1994. Estimates water balance of paleolake Qinghai in stable wet and warm period of Holocene. Advances in Water Science 5, 26–30.

Qin, B., 1997. Estimates of paleo-hydrological parameters and water balance of Qinghai Lake with energy-water balance model. Oceanologia et Limnologia Sinica 28, 611–616.

Please cite this article in press as: Rhode, D., et al., Paleoenvironmental and archaeological investigations at Qinghai Lake, western China:..., Quaternary International (2009), doi:10.1016/j.quaint.2009.03.004

Qin, B., Huang, Q., 1998. Evaluation of the climatic change impacts on the inland lake - a case study of Lake Qinghai, China. Climatic Change 39, 695–714.
Qu, Y.G., 1994. Water balance and forecasting of water level change in Qinghai Lake. Journal of Lake Science 6, 298–307 (in Chinese with English abstract).
Rhode, D., Zhang, H., Madsen, D.B., Gao, X., Brantingham, P.J., Ma, H., Olsen, J.W., 2007. Epipaleolithic/early Neolithic settlements at Qinghai Lake, western China. Journal of Archaeological Science 34, 600–612.
Shen, J., Liu, X., Wang, S., Matsumoto, R., 2005. Palaeoclimatic changes in the Qinghai Lake area during the last 18,000 years. Quaternary International 136, 131–140.
Shi, Y., Liu, X., Li, B., Yao, T., 1999. A very strong summer monsoon event during 30-40 kaBP in the Qinghai-Xizang (Tibet) Plateau and its relation to precessional cycle. Chinese Science Bulletin 44, 1851–1858.
Su, J., Wu, Y., Li, Q., Zhang, Y., Wen, X., 2005. Environmental evolution of the Jiuquan Basin and its relation to the uplift of the Qilian Mountains since the Quaternary. Acta Geoscientica Sinica 26, 443–448 (in Chinese with English abstract).
Tamburini, F., Adatte, T., Föllmi, K., Bernasconi, S.M., Steinmann, P., 2003. Investigating the history of East Asian monsoon and climate during the last glacial-interglacial period (0–140000 years): mineralogy and geochemistry of ODP Sites 1143 and 1144, South China Sea. Marine Geology 201, 147–168.
Vandenberghe, J., Renssen, H., van Huissteden, K., Nugteren, G., Konert, M., Lu, H., Dodonov, A., Buylaert, J.P., 2006. Penetration of Atlantic westerly winds into Central and East Asia. Quaternary Science Reviews 25, 2380–2389.
Walker, K.F., 1993. A Management Plan for the Naked Carp Fishery of Qinghai Lake. United Nations Development Program, Food and Agriculture Organization Report CPR/88/077. Rome.
Wang, S.M., Li, J.R., 1991. Lacustrine sediments an indicator of historical climatic variation, the case of Lakes Qinghai and Daihai. Chinese Science Bulletin 36, 1364–1368 (in Chinese).
Wang, S.M., Shi, Y.F., 1992. Review and discussion on the late Quaternary evolution of Qinghai Lake. Journal of Lake Sciences 4, 1–10 (in Chinese).
Wang, S.M., Wang, Y.F., Wu, R.J., Li, J.R., 1991. Qinghai Lake level fluctuation and climatic change since the last glaciation. Chinese Journal of Oceanology and Limnology 9, 179–183 (in Chinese).
Wang, Y., Cheng, H., Edwards, R.L., An, Z., Wu, J., Shen, C., Dorale, J., 2001. A high-resolution absolute-dated late Pleistocene monsoon record from Hulu Cave, China. Science 294, 2345–2348.
Wang, Y., Cheng, H., Edwards, R.L., He, Y., Kong, X., An, Z., Wu, J., Kelly, M.J., Dykoski, C.A., Li, X., 2005. The Holocene Asian Monsoon: Links to Solar Changes and North Atlantic Climate. Science 308, 854–857.
Wang, Y., Wang, X., Xu, Y., Zhang, C., Li, Q., Tseng, Z.J., Takeuchi, G., Deng, T., 2008. Stable isotopes in fossil mammals, fish and shells from Kunlum Pass Basin, Tibetan Plateau: Paleo-climatic and paleo-elevation implications. Earth and Planetary Science Letters 270, 73–85.
Xu, H., Li, A., Tan, L., An, Z., 2006. Stable isotopes in bulk carbonates and organic matter in recent sediments of Lake Qinghai and their climatic implications. Chemical Geology 235, 262–275.
Yan, H.Y., Jia, S.F., 2003. Water balance and water resources allocation of Qinghai Lake. Journal of Lake Science 15, 35–40 (in Chinese with English abstract).
Yan, J.P., Hinderer, M., Einsele, G., 2002. Geochemical evolution of closed-basin lakes: general model and application to Lakes Qinghai and Turkana. Sedimentary Geology 148, 105–122.
Yang, B., Shi, Y., Braeuning, A., Wang, J., 2004. Evidence for a warm-humid climate in arid northwestern China during 30–40 ka BP. Quaternary Science Reviews 23, 2537–2548.
Yang, X., Preusser, F., Radtke, U., 2006. Late Quaternary environmental changes in the Taklamakan Desert, western China, inferred from OSL-dated lacustrine and aeolian deposits. Quaternary Science Reviews 25, 923–932.
Yu, J.Q., 2005. Lake Qinghai, China: A multi-proxy investigation on sediment cores for the reconstructions of paleoclimate and paleoenvironment since the Marine Isotope Stage 3. Dissertation, Faculty of Materials and Geoscience, Technical University of Darmstadt.
Yu, J.Q., Kelts, K.R., 2002. Abrupt changes in climate conditions across the late-glacial/Holocene transition on the N.E. Tibet-Qinghai Plateau: evidence from Lake Qinghai. China. Journal of Paleolimnology 28, 195–206.
Yuan, B.Y., Chen, K., Ye, S.J., 1990. Origin and evolution of Lake Qinghai. Quaternary Sciences 3, 233–243 (in Chinese).
Yuan, D., Cheng, H., Edwards, R.L., Dygoski, C.A., Kelly, M.J., Zhang, M., Qing, J., Lin, Y., Wang, Y., Wu, J., Dorale, A., An, Z., Cai, Y., 2004. Timing, duration, and transitions of the last interglacial Asian Monsoon. Science 304, 575–578.
Zhang, H.C., Peng, J.L., Ma, Y.Z., Chen, G.J., Feng, Z.D., Li, B., Fan, H.F., Chang, F.Q., Lei, G.L., Wünnemann, B., 2004a. Late Quaternary palaeolake levels in Tengger Desert, NW China. Palaeogeography, Palaeoclimatology, Palaeoecology 211, 45–58.
Zhang, Z., Wang, S., Wu, X., Jiang, F., Li, X., 2004b. Evidence of a geological event and environment change in the catchment area of the Yellow River at 0.15 Ma. Quaternary International 117, 35–40.
Zhou, D.J., Ma, H.Z., Gao, D.L., Ma, W.D., Tan, H.B., Xu, L.M., 2004. Geochemical characteristics and climate environmental significance of Holocene loess on south Qinghai Lake shore. Journal of Desert Research 24, 144–148.

Please cite this article in press as: Rhode, D., et al., Paleoenvironmental and archaeological investigations at Qinghai Lake, western China:..., Quaternary International (2009), doi:10.1016/j.quaint.2009.03.004